Activity-Dependent Regulation of $[Ca^{2+}]_i$ in Avian Cochlear Nucleus Neurons: Roles of Protein Kinases A and C and Relation to Cell Death

Lance Zirpel, William R. Lippe and Edwin W Rubel

J Neurophysiol 79:2288-2302, 1998.

Activity-Dependent Regulation of $[Ca^{2+}]_i$ in Avian Cochlear Nucleus Neurons: Roles of Protein Kinases A and C and Relation to Cell Death

LANCE ZIRPEL, WILLIAM R. LIPPE, AND EDWIN W RUBEL
The Virginia Merrill Bloedel Hearing Research Center and The Department of Otolaryngology—Head and Neck Surgery, University of Washington School of Medicine, Seattle, Washington 98195

Zirpel, Lance, William R. Lippe, and Edwin W Rubel. Activity-dependent regulation of $[Ca^{2+}]_i$ in avian cochlear nucleus neurons: roles of protein kinases A and C and relation to cell death. *J. Neurophysiol.* 79: 2288–2302, 1998. Neurons of the cochlear nucleus, nucleus magnocellularis (NM), of young chicks require excitatory afferent input from the eighth nerve for maintenance and survival. One of the earliest changes seen in NM neurons after deafferentation is an increase in intracellular calcium concentration ($[Ca^{2+}]_i$). This increase in $[Ca^{2+}]_i$ is due to loss of activation of metabotropic glutamate receptors (mGluR) that activate second-messenger cascades involved in $[Ca^{2+}]_i$ regulation. Because mGluRs are known to act via the phospholipase C and adenylate cyclase signal transduction pathways, the goal of this study was to determine the roles of protein kinases A (PKA) and C (PKC) activities in the regulation of NM neuron $[Ca^{2+}]_i$ by eighth nerve stimulation. Additionally, we sought to determine the relationship between increased $[Ca^{2+}]_i$ and cell death as measured by propidium iodide incorporation. $[Ca^{2+}]_i$ of individual NM neurons in brain stem slices was monitored using fura-2 ratiometric fluorescence imaging. NM field potentials were monitored in experiments in which the eighth nerve was stimulated. Five hertz orthodromic stimulation maintained NM neuron $[Ca^{2+}]_i$ at ~110 nM for 180 min. In the absence of stimulation, NM neuron $[Ca^{2+}]_i$ increased steadily to a mean of 265 nM by 120 min. This increase was attenuated by superfusion of PKC activators phorbol-12,13-myristate acetate (100 nM) or dioctanoylglycerol (50 μM) and by activators of PKA: 1 mM 8-bromoadenosine-3′,5′-cyclophosphate sodium (8-Br-cAMP), 50 μM forskolin or 100 μM Sp-adenosine 3′,5′-cyclic monophosphothioate triethylamine. Inhibition of PKA (100 μM Rp-cAMPS) or PKC (50 nM bisindolymaleimide or 10 μM U73122) during continuous orthodromic stimulation resulted in an increase in NM neuron $[Ca^{2+}]_i$ that exceeded 170 and 180 nM, respectively, by 120 min. Nonspecific kinase inhibition with 1 μM staurosporine during stimulation resulted in an $[Ca^{2+}]_i$ increase that was greater in magnitude than that seen with either PKA or PKC inhibition alone, equal to that seen in the absence of stimulation, but much smaller than that seen with inhibition of mGluRs. In addition, manipulations that resulted in a $[Ca^{2+}]_i$ increase ≥250 nM resulted in an increase in number and percentage of propidium iodide-labeled NM neurons. These results suggest that eighth nerve activity maintains $[Ca^{2+}]_i$ of NM neurons at physiological levels in part via mGluR-mediated activation of PKA and PKC and that increases in $[Ca^{2+}]_i$ due to activity deprivation or interruption of the PKA and PKC $[Ca^{2+}]_i$ regulatory mechanisms are predictive of subsequent cell death.

INTRODUCTION

Neurons of the avian cochlear nucleus, nucleus magnocellularis (NM), depend on afferent eighth nerve activity for maintenance and survival. Removal of this input results in the death of 20–40% of the neurons, whereas the surviving neurons display profound morphological, metabolic, and physiological changes (reviewed in Rubel et al. 1990). One of the earliest changes observed in NM neurons after deafferentation is an increase in intracellular calcium concentration ($[Ca^{2+}]_i$) (Zirpel and Rubel 1996a; Zirpel et al. 1995a). This $[Ca^{2+}]_i$ increase is prevented by activation of one or more subtypes of metabotropic glutamate receptors (mGluR) (Zirpel and Rubel 1996a). NM neurons express mGluRs that are linked to two well-characterized mGluR-mediated signal transduction systems (reviewed in Zirpel et al. 1997). The first mGluR effect characterized in NM is activation of the phospholipase C pathway, which generates IP_3, liberates Ca^{2+} from intracellular stores, and presumably activates protein kinase C (PKC). The second mGluR effect characterized in NM neurons is the activation of the adenylate cyclase (AC) pathway, which generates adenosine 3′,5′-cyclophosphate sodium (cAMP), activates protein kinase A (PKA) and modulates Ca^{2+} influx through L-type channels, Ca^{2+} influx through ionotropic glutamate receptor (iGluR) channels, and Ca^{2+} release from intracellular stores (Lachica et al. 1995; Zirpel et al. 1997).

Strict regulation of $[Ca^{2+}]_i$ has been shown to be critical for the health and survival of neurons (Carafoli 1987; Collins et al. 1991; Franklin and Johnson 1992; Kennedy 1989; Siesjö 1989). Deregulation or loss of $[Ca^{2+}]_i$ homeostasis is toxic to neurons (Ghosh and Greenberg 1995; Koike et al. 1989; Mills and Kater 1990) and is implicated in a number of neuropathological conditions including ischemia, excitotoxicity, and anoxia (reviewed in Choi 1992) as well as Alzheimer's disease (Furukawa and Mattson 1995). PKA and PKC have been shown to be important to neuronal $[Ca^{2+}]_i$ regulation (Erausquin et al. 1990; Kikkawa et al. 1986; Wang et al. 1991) and survival (Kaiser and Lipton 1990; Wakade et al. 1988).

We have shown previously that NM neurons express one or more subtypes of mGluR linked to the phospholipase C (PLC)/PKC and AC/PKA signal transduction cascades and that NM neurons depend on activation of these mGluRs to maintain stable $[Ca^{2+}]_i$ homeostasis; inhibiting mGluR function with 1 mM (R,S)-α-methyl-4-carboxyphenylglycine (MCPG) results in a rapid and large increase in $[Ca^{2+}]_i$ (Zirpel and Rubel 1996a). Because it is widely accepted that PKC and PKA activities are important for both $[Ca^{2+}]_i$ regulation and cell survival and that loss of $[Ca^{2+}]_i$ homeo-

stasis is toxic to neurons, the goal of this study was to examine the roles of PKC and PKA in activity-dependent mGluR-mediated $[Ca^{2+}]_i$ regulation in NM neurons. In addition, we sought to determine the relationship between this $[Ca^{2+}]_i$ regulation and indicators of deafferentation-induced cell death. These results have been reported previously in abstract form (Zirpel and Rubel 1996b).

METHODS

Cochlea removals

Cochlea removals were performed on 17- to 19-day-old chick embryos as previously described (Lippe 1994; Zirpel et al. 1995a). The head of the embryo was pulled out through a small hole in the egg shell, lidocaine was applied to the right ear canal region, and the surrounding tissue was dissected away. A large incision was made in the tympanic membrane exposing the columella, which then was removed using fine forceps. A small glass suction pipette was inserted through the oval window, and the cochlea was removed by aspiration. The wound was packed with Gelfoam, the head of the embryo was replaced in the egg and the egg placed in a humidified incubator at 37°C. The embryos were allowed to recover for 1 or 3 h after which time they were decapitated and brain stem slices were acquired and labeled with propidium iodide as described in the following section.

Tissue preparation

Brain stem slices were obtained from 17- to 19-day-old chick embryos as previously described (Zirpel and Rubel 1996a; Zirpel et al. 1995b). A thick coronal section containing the entire brain stem was obtained from the decapitated embryo. The cerebellum and optic tectum were dissected free, and the remaining brain stem tissue was immersed in a 4% agarose solution. When the agarose solidified, 300-μm-thick coronal sections containing bilateral NM were acquired using a tissue slicer. All manipulations were performed in oxygenated artificial cerebrospinal fluid (ACSF). The slices then were allowed to equilibrate to room temperature in oxygenated ACSF for 45 min, after which time they were placed in an oxygenated ACSF solution containing 5–10 μM fura-2 AM (Molecular Probes, Eugene, OR), 1.7% anhydrous dimethylsulfoxide (DMSO; Aldrich Chemical, Milwaukee, WI), and 0.03% Pluronic (Molecular Probes) for 30 min. Slices then were placed in a Teflon imaging chamber (Ince et al. 1985) and continuously superfused with oxygenated ACSF at a rate of 3 ml/min. All experiments were performed at room temperature.

Electrophysiology

Techniques for stimulating and recording in chick brain stem slices in vitro have been described previously (Hyson and Rubel 1989; Zirpel and Rubel 1996a). Twisted Teflon-coated silver wires (Medwire, Mt. Vernon, NY) comprised the bipolar stimulating electrode. Stimulation consisted of 1–4 mA, 20-μs pulses delivered at a rate of 5 Hz. Recording electrodes were pulled from borosilicate glass (World Precision Instruments, Sarasota, FL) to resistances of 1–5 MΩ and filled with ACSF. To orthodromically stimulate NM, the stimulating electrode was placed on the eighth nerve (VIIIth n.) root lateral to NM. The VIIIth nerve is the sole excitatory input to NM (Born et al. 1991) and is a glutamatergic synapse (Jackson et al. 1985; Martin 1985; Nemeth et al. 1983; Raman and Trussell 1992; Zhou and Parks 1992a,b). Field potentials were monitored in all stimulated slices by placing a recording electrode in NM. Responses were amplified (WPI M-707), displayed on an oscilloscope (Tektronix, Beaverton, OR) and recorded photographically. Traces were scanned into Adobe Photoshop (Adobe Systems, Mountain View, CA) and optically averaged. Amplitude measurements were made in Freehand (Macromedia, San Francisco, CA).

Fura-2 calcium imaging

Fluorometric imaging techniques using this preparation have been described previously (Zirpel and Rubel 1996a; Zirpel et al. 1995). Slices containing fura-2–loaded NM neurons were placed in the imaging chamber on the stage of a Nikon Diaphot inverted microscope and alternately excited with 340 and 380 nm wavelengths of light attenuated to 3% by an in-line 1.5 neutral density filter. Fura-2 fluorescence emission was obtained at 510 nm by an intensified CCD (Hamamatsu, Japan) using a ×40 fluor oil immersion lens (Nikon) and a 480-nm long-pass barrier filter. Paired 340/380 fluorescence ratio images were acquired every 3, 10, 30, or 180 s. Exposure time for each excitation wavelength was 750 ms.

Individual NM neurons were identified easily in these slices and were randomly chosen for analysis only if the ratio image (340/380) of any given cell was >50 pixels. Cells were outlined for analysis using Image-1/Fluor software (Universal Imaging, West Chester, PA). From 5 to 20 NM neurons per slice were analyzed with the average slice, yielding nine NM neurons for analysis. Ratios (340:380) were converted to intracellular calcium concentrations ($[Ca^{2+}]_i$) by the Image-1/Fluor software with an external high-low calibration technique (Grynkiewicz et al. 1985). This calibration technique employed several in vitro solutions ranging in calcium concentrations from nominally calcium free to 36 μM free calcium (Molecular Probes) and 100 μM pentapotassium fura-2 under identical imaging conditions as used in the experiments. On-line ratio values were converted to calcium concentrations by interpolation from this curve. The Kd of fura-2 was assumed to be 224 nM (Grynkiewicz et al. 1985). Neurons with initial $[Ca^{2+}]_i$ of ≥250 nM were assumed to have been injured in the tissue preparation and were excluded from the data acquisition process. The majority of slices contained no NM neurons with $[Ca^{2+}]_i$ this high, and few slices contained more than four cells with high $[Ca^{2+}]_i$: average = 2% of all cells in all slices showed an initial $[Ca^{2+}]_i$ this high. Cells chosen for analysis were monitored continuously for the duration of the experiment; no cells were added during the course of the experiment, and cells that were chosen initially but subsequently exhibited a complete loss of fluorescent signal were excluded from analysis. Loss of fura-2 fluorescence is reported to indicate cell death (Johnson et al. 1994).

Data analysis

$[Ca^{2+}]_i$ levels for neurons within a given slice were averaged at ~5-min intervals. For statistical analyses, the mean $[Ca^{2+}]_i$ for all cells analyzed in a given slice at a particular time point was treated as a single observation ($n = 1$). Thus ns for each statistical comparison were the number of slices in a treatment group, except where otherwise noted. Data are presented as means ± SE. The total number of neurons is presented followed by n = number of slices. The time-related change of $[Ca^{2+}]_i$ was compared between treatment groups of interest by examining the interaction term in the appropriate two-way analysis of variance (ANOVA, treatment-by-time with repeated measures on the time factor). The values reported in the results are for the interaction term. Data were plotted using Excel (Microsoft, Redmond, WA) and Cricket Graph III (Cricket Software, Malvern, PA). Two-way ANOVA and t-tests were performed using Statview (Abacus Concepts, Berkeley, CA) and SAS/STAT (SAS Institute, Cary, NC).

Cell viability

Immediately after fura-2 experiments, slices were incubated in situ in the imaging chamber for 30 min in 1 ml ACSF containing

1.5 μM propidium iodide (PI). Images of NM then were acquired using Image-1 software (Universal Imaging) and processed in Photoshop (Adobe Systems) or NIH Image 1.60 (public domain software developed at the U.S. National Institutes of Health and available on the internet at http://rsb.info.nih.gov/nih-image/). Excitation was achieved using a 535-nm filter and emissions were collected using a 600-nm long-pass filter. All PI-labeled NM neurons within a field of view were counted by an observer with no knowledge of the treatment. Cells were counted in a 200 $\times$ 200 μm field of view. PI-labeled glia were discerned easily from PI-labeled (PI+) NM neurons and were excluded from counts (Fig. 2*A*). The total number of NM neurons in each field of view analyzed for PI labeling was obtained by counting cells in the same field of view under Köhler illumination or fura-2 excitation. The PI+ neuron counts for different treatment groups were compared using one-factor ANOVA and Fisher's protected least significant difference (PLSD) post hoc test.

For stimulation experiments in which fura-2 imaging was not performed, slices were incubated in oxygenated ACSF containing 1.5 μM PI for 30 min immediately after the defined period of stimulation (1 or 3 h). Slices obtained from brains of chicks that had undergone in vivo cochlea removal were allowed to equilibrate for 45 min in room-temperature, oxygenated ACSF before undergoing PI labeling as described above. All slices then were washed three times for 2 min in fresh ACSF and placed in an imaging chamber mounted on a Nikon Diaphot microscope. PI images were acquired using a BioRad MRC 1024 laser confocal scanning microscope. Excitation (535 nm) was achieved with the yellow line (568 nm) of a Ar/Kr laser. Emission images (620 nm) were collected through a 585-nm long-pass filter with either a $\times$10 or $\times$20 Fluor objective (Nikon). Images were slow-scanned using a Kalman filter (factor of 3) and saved on hard drive and optical disk. Images were processed in Adobe Photoshop and NIH Image. PI-labeled NM neurons in a 200 $\times$ 200 μm field were counted in NM on both sides of each slice by an observer with no knowledge of treatment group and compared using a paired two-tailed *t*-test. The total number of cells in any given field of view was obtained from images of the same focal plane acquired by the photomultiplier tube under standard light transmission microscopy conditions. Numbers presented are raw means $\pm$ SE of the mean followed parenthetically by the percentage of mean total NM neurons.

All slices, regardless of experiment type, were treated identically with regard to preparation time. Complete preparation time was ~90 min and, because it was identical for all slices, is not reported in the data presentation. Times reported are those that were variable for different treatment groups in any given experimental paradigm (e.g., survival time after cochlea removal). Thus the absolute times between cochlea removal and PI analysis are ~90 min longer than the times reported in RESULTS.

Drugs, chemicals, and media

Slices were superfused continuously at a rate of ~3 ml/min with oxygenated ACSF consisting of (in mM) 130 NaCl, 3 KCl, 2 $CaCl_2$, 2 $MgCl_2$, 26 $NaHCO_3$, 1.25 NaH_2PO_4, and 10 glucose.

MCPG, 8-bromoadenosine-cAMP (Br-cAMP), Sp-adenosine 3′,5′-cyclic monophosphothioate triethylamine (Sp-cAMPS), Rp-cAMPS, phorbol-12-myristate-13-acetate (PMA), 4-α-phorbol-PMA (4-α-PMA), forskolin, and 1,9-dideoxy-forskolin were obtained from Research Biochemicals, (Natick, MA). Bisindolylmaleimide, staurosporine, U73122, U73343, and 1,2-dioctanoyl-*sn*-glycerol (DOG) were acquired from Calbiochem (San Diego, CA). Glutamate and propidium iodide were obtained from Sigma Chemical Company (St. Louis, MO). All other reagents were of analytic grade. Stock solutions of staurosporine, PMA, 4α-PMA, bisindolymaleimide, DOG, forskolin, 1,9-dideoxy-forskolin, U73122, and U73343 were in DMSO and diluted to working concentrations with ACSF. Stock solution of propidium iodide was in distilled H_2O. All other pharmaceuticals were dissolved in ACSF. All working solutions were prepared within 24 h of use.

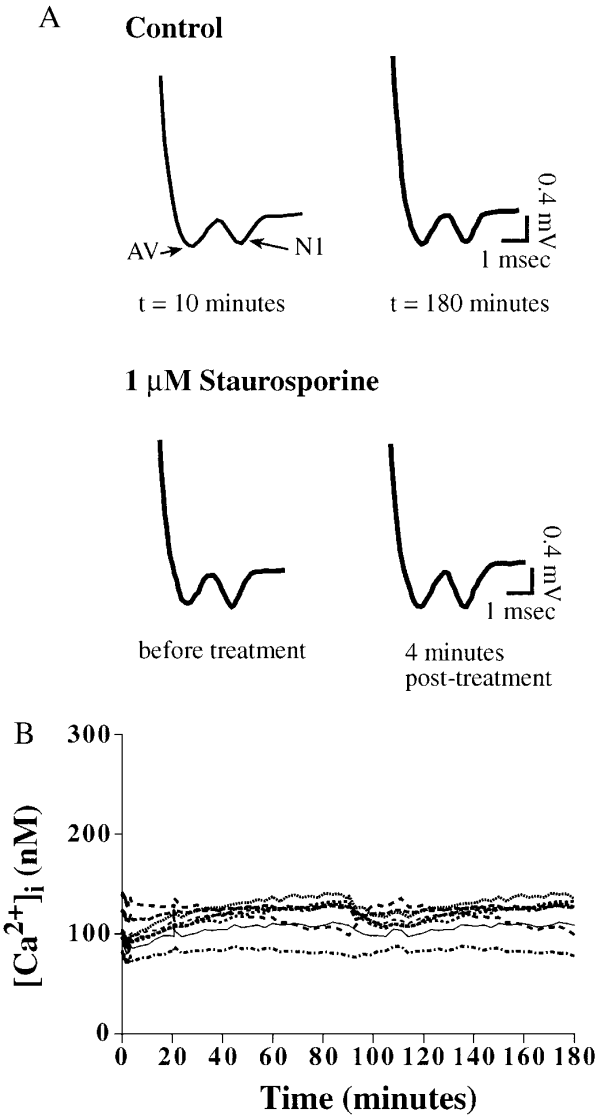

FIG. 1. *A*: nucleus magnocellularis (NM) field potentials in response to 5-Hz stimulation of the VIIIth nerve. *Top*: representative of NM field potentials in control conditions. AV, afferent volley; N1, postsynaptic NM response. *Left*: acquired 10 min after initiation of the stimulus; *right*: acquired after 3 h of stimulation and imaging. Note that there is no significant change in the amplitude of response. *Bottom*: 4 min after beginning superfusion of artificial cerebrospinal fluid (ACSF) containing 1 μM staurosporine, the amplitude of both AV and N1 are potentiated. Initial deflection on all traces is stimulus artifact. *B*: intracellular Ca^{2+} levels of 8 NM neurons receiving 5-Hz stimulation of the VIIIth nerve. Note that the $[Ca^{2+}]_i$ is stable at 100 nM for the duration of the 180-min experiment. $t = 0$ is ~90 min from time of animal euthanization.

RESULTS

Electrophysiology

Figure 1*A* shows representative traces of NM field potentials produced by stimulation of the VIIIth nerve. Stimulus levels were adjusted to produce field potentials that were ~90% of the maximum response amplitude recorded at the initiation of recording. The stimulation rate for all experiments was 5 Hz. This frequency of stimulation has been shown to

TABLE 1. *N1 amplitude of NM field potentials before and after pharmacological treatment during 5-Hz orthodromic stimulation*

Preamplitude, mV	Treatment	Postamplitude, mV	Post/Pre Ratio	*n*
0.78 ± 0.16	Control (180 mins)	0.81 ± 0.17	1.04	5
0.68 ± 0.05	50 nM bisindoly	0.70 ± 0.04	1.03	4
0.80 ± 0.04	100 μM Rp-cAMPS	0.84 ± 0.06	1.05	4
0.93 ± 0.13*	1 μM staurosporine	1.10 ± 0.12	1.18	4
0.83 ± 0.13†	Stauro + 1 mM MCPG	1.03 ± 0.13	1.24	3
0.48 ± 0.07	10 μM U73122	0.52 ± 0.09	1.08	3
0.85 ± 0.05	10 μM U73343	0.83 ± 0.08	0.98	2

Values expressed are means ± SE. * and † = significant pre-post difference paired two-tail *t*-test: *$P = 0.035$, †$P < 0.0001$. All other comparisons are nonsignificant ($P > 0.05$). NM, nucleus magnocellularis; Rp-cAMPS, Rp-adenosine 3′,5′-cyclic monophosphothioate triethylamine; MCPG, (R,S)-α-methyl-4-carboxyphenylglycine.

reliably prevent decreases in protein synthesis (Hyson and Rubel 1989) that otherwise occur in slice preparations without orthodromic stimulation, and to maintain stable $[Ca^{2+}]_i$ levels in NM neurons (Zirpel and Rubel 1996a). Although this preparation can follow higher stimulation rates, responses tend to be more variable during a long period, thus preventing precise measurements of activity. Thus we chose to use 5-Hz stimulation in all of the experiments reported here.

Response amplitudes ranged between 0.3 and 1.4 mV and did not vary significantly during the course of 3-h experiments (Fig. 1*A;* Table 1). With the exception of staurosporine, none of the compounds used in this study affected magnitude or latency of recorded field potentials (Table 1). This was somewhat surprising because it is known that PKA activity modulates L-type Ca^{2+} channels in NM neurons (Lachica et al. 1995) and that PKC and PKA activators modulate multiple ion channels and currents in other cell types (Greengard et al. 1991; Kelso et al. 1992; Madison and Nicoll 1986; Malenka et al. 1986; Miller 1986; Wang et al. 1991). However, field potential recordings may not reveal subtle changes in ion fluxes related to synaptic transmission, especially Ca^{2+} currents that are much smaller than Na^+ and K^+ currents (Otis et al. 1995; Raman and Trussell 1992). Bath application of 1 μM staurosporine and the combination of 1 μM staurosporine + 1 mM MCPG, significantly potentiated the amplitude of both the primary afferent volley (AV) (data not shown) and N1 components of the NM field potential within 4 min of application (Table 1, Fig. 1*A;* see *mGluRs, Kinases and NM Neuron* $[Ca^{2+}]_i$ *Regulation*), suggesting that there is an ongoing level of kinase activity directed at the ion channels. MCPG alone does not affect field potential amplitude or latency (Zirpel and Rubel 1996a).

Figure 1*B* shows that 5-Hz stimulation of the VIIIth nerve maintains stable NM neuron $[Ca^{2+}]_i$ at physiological levels for ≤3 h.

Cell viability

NM neurons show a significant increase in $[Ca^{2+}]_i$ within 1 h of an in vivo cochlea removal, and $[Ca^{2+}]_i$ remains elevated for ≥12 h (Zirpel et al. 1995a). To determine if this increase in $[Ca^{2+}]_i$ relates to NM neuron death, embryos underwent unilateral cochlea removal and were allowed to survive for 1 or 3 h. Live slices containing bilaterally symmetric NM then were labeled with PI. PI is a fluorescent DNA dye that is excluded from healthy cells but incorporated into the nucleus of dead *or* dying cells (London et al.

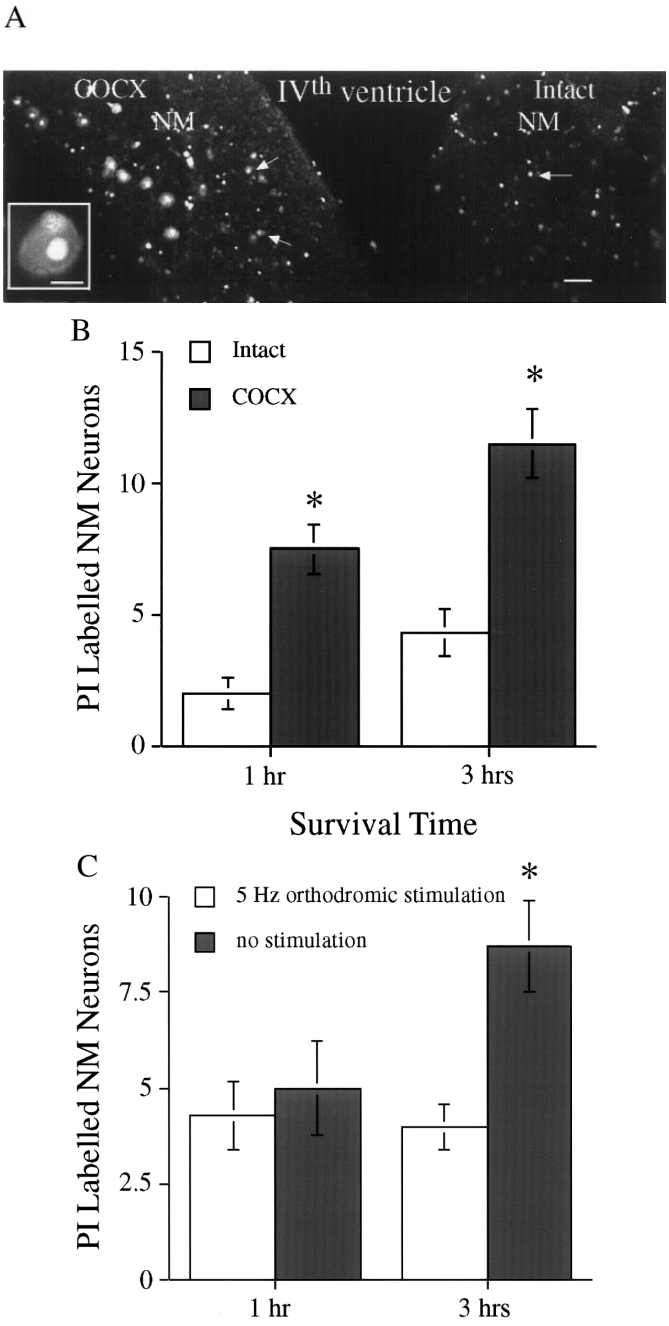

FIG. 2. Propidium iodide (PI) labeling of NM neurons is determined by synaptic activity in vivo and in vitro. *A*: confocal image of a PI labeled slice 3 h after an in vivo cochlea removal. *Left*: ipsilateral to cochlea removal (COCX); note the higher number of labeled neurons in NM compared with contralateral (intact) NM. It is easy to see that glia (→) can be differentiated readily from neurons. *Inset*: higher power of an individual NM neuron labeled with PI. Note that PI is incorporated into the nucleus of the neuron. Scale bar = 50 μm; *inset* scale bar = 20 μm. *B*: histograms showing mean number of PI-labeled NM neurons ipsi- and contralateral to an in vivo cochlea removal at 1 ($n = 4$ slices)- and 3 ($n = 4$ slices)-h survival times. *$P < 0.05$, paired 2-tail *t*-test. Error bars represent the standard error of the mean. *C*: histograms showing the number of PI-labeled NM neurons on stimulated and unstimulated sides of an in vitro slice after 1 ($n = 3$ slices) and 3 ($n = 3$ slices) hours of stimulation. *$P = 0.0339$, paired 2-tailed *t*-test. Error bars represent the standard error of the mean.

1989; Nicoletti et al. 1991; Wilde et al. 1994). Figure 2*A* shows that the labeled NM neurons are distinguished easily from labeled glia. The *inset* in Fig. 2*A* further shows that PI indeed has been incorporated in to the nucleus of the NM neuron. PI-labeled NM neurons were counted and compared between the intact and deafferented NM nuclei of each slice at the different survival times. Figure 2, *A* and *B*, shows the results of these experiments. The mean *total* number of NM neurons per field of view in all slices analyzed is 30.23 ± 2.17 (n = 72 slices). One hour after cochlea removal, the ipsilateral NM shows significantly more (7.5 ± 0.9; 24%) PI-labeled neurons than the contralateral intact NM (2.0 ± 0.6; 7%) (Figure 2*B; P* = .0079, paired *t*-test, n = 4 slices), a 17% increase. Mean NM neuron $[Ca^{2+}]_i$ is 247 ± 29 nM 1 h after cochlea removal (Zirpel et al. 1995a). Because it is unlikely that NM neurons would be dead only 60 min after cochlea removal, we presume that the PI-labeled NM neurons are those that eventually will die, similar to the ''ghost'' cells reported by Steward and Rubel (1985) after measuring protein synthesis after cochlea removal, and are therefore either dead or *in the process of dying*. However, given that these measurements are taken from an in vitro slice preparation, it is not surprising that a few cells (7–14% of total number) are labeled with PI even on the intact side. These cells presumably have been damaged during the dissection and preparation process and represent an unavoidable level of cell death associated with an in vitro preparation.

Three hours after cochlea removal, the difference in number of PI-labeled NM neurons between the cochlea removal side (COCX) and the intact side was still significant [11.5 ± 1.3 (38%) vs. 4.3 ± 0.9 (14%), respectively; Fig. 2*B; P* = 0.02, paired *t*-test, n = 4 slices]. Three hours after cochlea removal, mean NM neuron $[Ca^{2+}]_i$ was 311 ± 28 nM (Zirpel et al. 1995a). In two animals that were allowed to survive for 24 h after cochlea removal, there was no significant difference in number of PI-labeled NM neurons between COCX and intact sides (data not shown, P = 0.9). Cell bodies of dying neurons still can be seen 24 h after cochlea removal (Born and Rubel 1985) but show no protein synthesis (Steward and Rubel 1985) nor Nissl staining (Born and Rubel 1985). Therefore PI labeling in the intact and deafferented NM may not differ at 24 h survival because the NM neurons that are going to die essentially have done so (Born and Rubel 1985) and the DNA has been degraded by Ca^{2+}-dependent endonucleases (Cohen and Duke 1984; Wyllie et al. 1984). Interestingly, a larger number of glia cells on the deafferented side of the brain stems also incorporated PI, though this was not systematically quantified.

VIIIth nerve stimulation of an in vitro slice maintains stable NM neuron $[Ca^{2+}]_i$ at baseline levels for ≤3 h (Fig. 1*B*) (Zirpel and Rubel 1996a). However, termination of that stimulation results in a gradual $[Ca^{2+}]_i$ increase that begins within 20 min (Zirpel and Rubel 1996a). To relate this in vitro $[Ca^{2+}]_i$ increase to cell death, slices were stimulated unilaterally for 1 or 3 h and then labeled with PI. PI-labeled NM neurons were counted and compared between the stimulated and unstimulated NM in each slice. Figure 2*C* shows the results of these experiments. After 1 h of unilateral stimulation, the average number of PI-labeled neurons in the stimulated NM was 4.3 ± 0.9 (14%), whereas the average number of PI-labeled neurons in the contralateral (unstimulated) side was 5.0 ± 1.2 (17%). These numbers are not significantly different (paired *t*-test, P = .1835, n = 3 slices). However, after 3 h of unilateral stimulation, the unstimulated NM shows significantly more PI-labeled neurons than the stimulated NM [8.7 ± 1.2 (29%) vs. 4.0 ± 0.6 (13%), P = .0339, n = 3 slices].

PKA and PLC in NM neuron $[Ca^{2+}]_i$ *regulation*

PROTEIN KINASE A. Pharmacological studies have shown that NM neurons express an mGluR that generates cAMP (reviewed in Zirpel et al. 1997), which presumably then activates PKA, which subsequently phosphorylates and modulates the activities of target proteins and enzymes. We previously have shown that this modulation includes inhibition of L-type voltage operated Ca^{2+} channels, inhibition of Ca^{2+} influx through ionotropic glutamate receptors, and inhibition of Ca^{2+} release from intracellular stores. In other cell types, PKA has been shown to be involved in cellular Ca^{2+} regulation (Fukayama et al. 1993) and modulation of ionotropic receptors (Greengard et al. 1991; Wang et al. 1991) and Ca^{2+} ATPases (Hawkins et al. 1995b). Thus it is likely that PKA plays a role in mGluR-mediated VIIIth nerve activity-dependent regulation of NM neuron $[Ca^{2+}]_i$. To test this hypothesis, PKA was either pharmacologically activated in the absence of stimulation or pharmacologically inhibited during VIIIth nerve stimulation while $[Ca^{2+}]_i$ was monitored.

Superfusing slices with ACSF containing the adenylate cyclase stimulator forskolin (50 μM) attenuated, but did not entirely prevent, (Fig. 3*A*, □, 47 neurons, n = 4 slices) the increase in $[Ca^{2+}]_i$ normally seen in unstimulated NM neurons (Fig. 3*A*, ◇, 52 neurons, n = 4 slices). Both control unstimulated and forskolin-treated unstimulated NM neurons exhibited normal $[Ca^{2+}]_i$ at the beginning of the experiments (100 ± 13 and 117 ± 7 nM, respectively). Control NM neurons showed an obvious increase in $[Ca^{2+}]_i$ after 45 min that continued for another 75 min, reaching an average final concentration of 271 ± 22 nM. Forskolin-treated NM neurons did not show a sharp increase like the control NM neurons, but showed a very slow, gradual increase that reached an average concentration of 163 ± 20 nM after 120 min. This effect is significantly different from the unstimulated control ($F_{(24,144)}$ = 20.04, P = 0.0001) as well. Superfusion of 50 μM 1,9-dideoxy-forskolin, an inactive form of forskolin that does not stimulate AC, had no effect on the $[Ca^{2+}]_i$ increase seen in unstimulated NM neurons (data not shown, 24 neurons, n = 2 slices).

Superfusing unstimulated slices with the cell permeable cAMP analog/PKA activator 8-Br-cAMP (1 mM) also significantly attenuated the $[Ca^{2+}]_i$ increase normally seen in the absence of stimulation (Fig. 3*A*, ○, 35 neurons, n = 4 slices). The mean $[Ca^{2+}]_i$ of NM neurons at the initiation of 8-Br-cAMP superfusion was 130 ± 13 nM. After 120 min, the $[Ca^{2+}]_i$ was 155 ± 19 nM. The effect of 8-Br-cAMP superfusion is also significantly different from the control unstimulated group ($F_{(24,144)}$ = 28.09, P = 0.0001) but not from the forskolin group ($F_{(24,144)}$ = 0.92, P = 0.5757). In one of the four 8-Br-cAMP experiments, addition of the PKA activator appeared to drive down the $[Ca^{2+}]_i$ from an approximate mean of 180 nM to an approximate mean of 150 nM during the first 60 min of the experiment (Fig. 3*A*, *inset*, traces from 8 NM

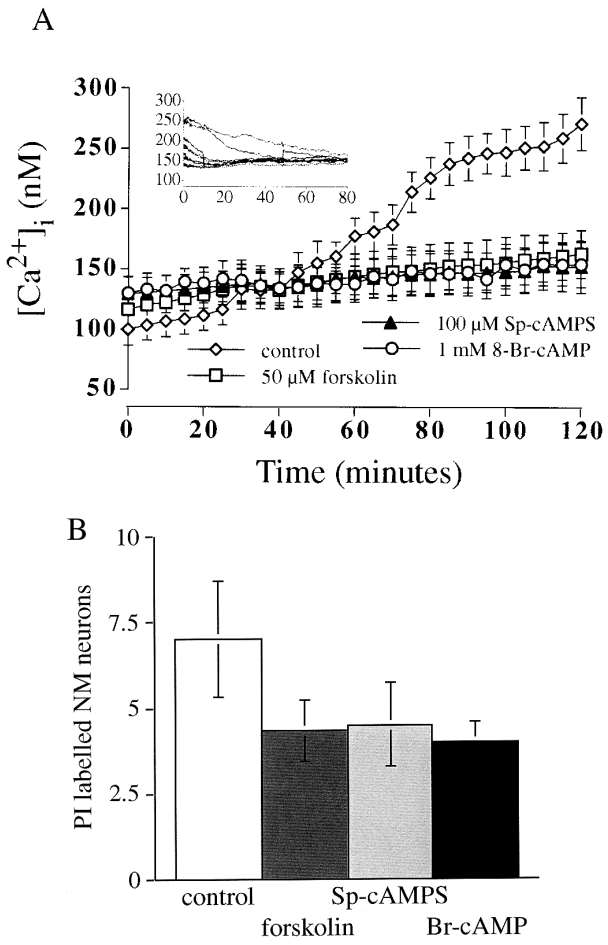

FIG. 3. Activators of protein kinase A (PKA) attenuate the $[Ca^{2+}]_i$ increase normally seen in unstimulated NM neurons. *A*: average $[Ca^{2+}]_i$ levels in unstimulated NM neurons in response to bath application of the following: ◇, control (ACSF only; 52 neurons, $n = 4$ slices); □, 50 μM forskolin, an adenylate cyclase activator that increases adenosine 3′,5′-cyclophosphate sodium (cAMP) concentrations (47 neurons, $n = 4$ slices); ○, 1 mM 8-bromoadenosine-3′,5′-cyclophosphate sodium (8-Br-cAMP), a cell permeable cAMP analog (35 neurons, $n = 4$ slices); and ▲, 100 μM Sp-adenosine 3′,5′-cyclic monophosphothioate triethylamine (Sp-cAMPS, 55 neurons, $n = 4$ slices), a cell permeable cAMP analog. *Inset*: $[Ca^{2+}]_i$ traces from 8 NM neurons in which application of Br-cAMP reduced the levels of $[Ca^{2+}]_i$ in all neurons. $t = 0$ is ~90 min from time of animal euthanization. *B*: histograms showing the number of PI-labeled NM neurons in each of the groups in *A*. Error bars represent standard error of the mean in both *A* and *B* and are <10 nM where not seen in *A*.

neurons). This effect was not observed in any of the other three 8-Br-cAMP experiments.

Sp-cAMPS is another cell permeable analog of cAMP that binds to the cyclic nucleotide binding region in the regulatory subunit of PKA and is resistant to degradation by phosphodiesterases (Kebabian 1992). NM neurons in unstimulated slices superfused with 100 μM Sp-cAMPS showed an attenuated, but not an entirely abolished, increase in $[Ca^{2+}]_i$ during 120 min (Fig. 3*A*, ▲, 55 neurons, $n = 4$ slices). NM neurons at the start of the experiments exhibited a mean $[Ca^{2+}]_i$ of 130 ± 5 nM. $[Ca^{2+}]_i$ increased gradually to a concentration of 153 ± 11 nM after 120 min. This increase is also significantly less than the control unstimulated ($F_{(24,144)} = 32.30$, $P = 0.0001$), but not from the forskolin ($F_{(24,144)} = 0.72$, $P = 0.8260$) or 8-Br-cAMP ($F_{(24,144)} = 0.25$, $P = 0.9999$) groups.

After the termination of the experiments discussed earlier and shown in Fig. 3*A*, the slices were analyzed for PI-labeled NM neurons. Figure 3*B* shows that slices superfused with 50 μM forskolin, 1 mM Br-cAMP, or 100 μM Sp-cAMPS tended to show fewer PI-labeled NM neurons than control (unstimulated) NM neurons. However, these differences were not statistically significant using a one-way ANOVA ($F_{(5,15)} = 1.890$, $P = 0.1647$).

To determine the contribution of PKA activity to the maintenance of normal NM neuron $[Ca^{2+}]_i$ conferred by VIIIth nerve activity, slices receiving 5-Hz stimulation were superfused with Rp-cAMPS while $[Ca^{2+}]_i$ was monitored. If PKA serves an important role in NM neuron $[Ca^{2+}]_i$ regulation, inhibition of PKA during continued orthodromic stimulation should disrupt the ability of VIIIth nerve activity to maintain physiological levels of intracellular Ca^{2+}. Rp-cAMPS is the diastereomer of Sp-cAMPS and is an antagonist of the interaction between cAMP and PKA (Kebabian 1992), thus serving as an antagonist of PKA activity. Slices were stimulated for 10 min to ensure stable baseline NM neuronal $[Ca^{2+}]_i$ and then superfused with ACSF containing 100 μM Rp-cAMPS. Figure 4*A* shows the $[Ca^{2+}]_i$ response of NM neurons in slices receiving 5-Hz orthodromic stimulation alone and those receiving stimulation while being superfused with Rp-cAMPS. Orthodromic stimulation maintained the NM neuron $[Ca^{2+}]_i$ at ~115 nM for 130 min (●, 63 neurons, $n = 5$ slices). NM neurons in slices receiving stimulation while being superfused with Rp-cAMPS showed two similar but distinct $[Ca^{2+}]_i$ changes. The first population comprised 81% (25 of 31 neurons in 4 slices) of the neurons observed and showed a small, slow increase in $[Ca^{2+}]_i$ that became evident after 50 min of Rp-cAMPS superfusion (Fig. 4*A*, ▽). These neurons exhibited an initial mean $[Ca^{2+}]_i$ of 121 ± 6 nM that increased to 155 ± 5 nM by 120 min. The remaining 19% of the neurons (6 of 31 neurons in 4 slices) showed a much more, rapid, erratic and larger $[Ca^{2+}]_i$ increase (Fig. 4*A*, △) after application of Rp-cAMPS during continued orthodromic stimulation. Interestingly, this subpopulation of NM neurons showed a higher mean initial $[Ca^{2+}]_i$ of 171 ± 17 nM. By 50 min after initiation of Rp-cAMPS superfusion, these neurons had reached a mean $[Ca^{2+}]_i$ of 243 ± 37 nM. The $[Ca^{2+}]_i$ continued to increase rapidly and erratically, reaching a mean final concentration of 338 ± 30 nM at 120 min. The combined mean $[Ca^{2+}]_i$ of both populations also is plotted in Fig. 4*A* (◆, 31 neurons, $n = 4$ slices). This population mean showed an initial $[Ca^{2+}]_i$ of 130 ± 5 nM that gradually increased to 196 ± 15 nM at 120 min. This increase is significantly different from the control stimulated group ($F_{(26,156)} = 13.12$, $P = 0.0001$). Due to the ''high-initial $[Ca^{2+}]_i$ neurons,'' this mean increase showed two large step-increases at 50 min (from 134 ± 23 to 157 ± 10 nM) and 100 min (from 173 ± 8 to 191 ± 16). Rp-cAMPS did not affect the magnitude or latency of NM field potentials in any experiment (Table 1).

Figure 4*B* shows that slices superfused with 100 μM Rp-cAMPS while receiving orthodromic stimulation tended to show a higher number of PI-labeled NM neurons than slices receiving orthodromic stimulation in normal ACSF; however, the difference was again not statistically significant (one-factor ANOVA, $F_{(5,12)} = 1.873$, $P = 0.1731$).

The results of these experiments suggest that PKA plays a significant role in VIIIth nerve activity-dependent, mGluR-

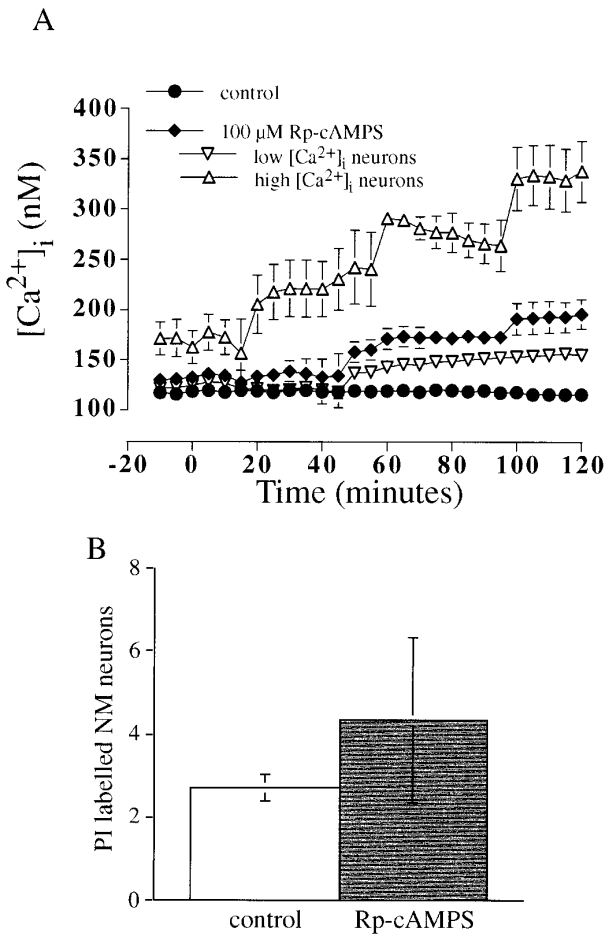

FIG. 4. Antagonism of PKA activity interrupts the ability of continuous orthodromic stimulation to maintain stable NM neuron $[Ca^{2+}]_i$. *A*: average NM neuron $[Ca^{2+}]_i$ in slices receiving continuous 5-Hz stimulation superfused with ACSF (●, 63 neurons, $n = 5$ slices; same data as in Fig. 3*A*) or 100 μM Rp-cAMPS (♦, 31 neurons, $n = 4$ slices). Response of NM neurons to Rp-cAMPS superfusion while receiving stimulation fell into 2 populations. NM neurons that exhibited high (>150 nM) initial $[Ca^{2+}]_i$, showed a rapid, stepwise increase in $[Ca^{2+}]_i$ (△, 6/31 neurons), whereas those with normal initial $[Ca^{2+}]_i$ showed a more gradual $[Ca^{2+}]_i$ increase (▽, 25/31 neurons). $t = 0$ is ~90 min from time of animal euthanization. *B*: histograms showing the number of PI-labeled NM neurons in slices superfused with 100 μM Rp-cAMPS while receiving 5-Hz orthodromic stimulation and control slices receiving 5-Hz orthodromic stimulation. Error bars represent standard error of the mean in both *A* and *B* and are <10 nM where not seen in *A*.

mediated regulation of NM neuron $[Ca^{2+}]_i$. Furthermore, it appears that inhibition of PKA disrupts the $[Ca^{2+}]_i$ homeostasis mechanisms of a subpopulation of NM neurons that exhibit an already elevated $[Ca^{2+}]_i$. However, these alterations in PKA activity and $[Ca^{2+}]_i$ homeostasis did not significantly increase the number of PI-labeled NM neurons.

PROTEIN KINASE C. Previous studies have shown that NM neurons express mGluRs that, on activation, stimulate the production of IP_3 (Zirpel et al. 1994) and cause Ca^{2+} release from intracellular stores (Zirpel et al. 1995b). These effects are presumably mediated through mGluR activation of PLC, which, in addition to the IP_3/Ca^{2+}-release effect, also generates diacylglycerol (DAG), which, together with free cytosolic Ca^{2+}, stimulates PKC (Nishizuka 1984, 1986). To determine the contribution of PKC activity to NM neuron $[Ca^{2+}]_i$ regulation, $[Ca^{2+}]_i$ was monitored in unstimulated slices while PKC was activated directly with the phorbol ester PMA and indirectly with a DAG analog, DOG. Conversely, in slices receiving 5-Hz stimulation, NM neuron $[Ca^{2+}]_i$ was monitored while PKC was inhibited with bisindolymaleimide and while PLC was inhibited with U73122. Employing U73122 is useful in that it not only blocks the generation of DAG and subsequent activation of PKC but also inhibits the generation of IP_3 and subsequent release of Ca^{2+} from internal stores (Grierson and Meldolesi 1995; Thompson et al. 1991). Thus any difference in NM neuron $[Ca^{2+}]_i$ regulation between inhibition of PKC and inhibition of PLC can be attributed to the IP_3 branch of this signal transduction system.

Figure 5*A* shows that superfusing unstimulated slices with ACSF containing 100 nM PMA or 50 μM DOG prevented the $[Ca^{2+}]_i$ increase normally seen in unstimulated NM neurons. In the absence of stimulation, NM neuron $[Ca^{2+}]_i$ increased from a mean of 100 ± 13 to 271 ± 22 nM after

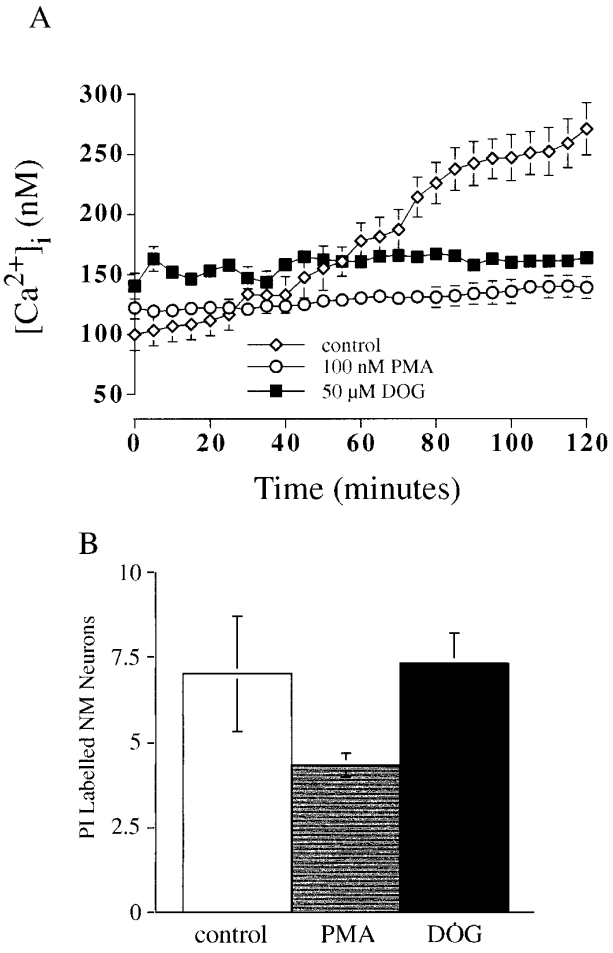

FIG. 5. Activation of PKC attenuates the NM neuron $[Ca^{2+}]_i$ increase seen in the absence of stimulation. *A*: mean NM neuron $[Ca^{2+}]_i$ in the absence of stimulation (◇, 52 neurons, $n = 4$ slices; same data as in Fig. 3*A*), while being superfused with ACSF containing 100 nM of the PKC-activating phorbol ester phorbol-12-myristate-13-acetate (PMA, ○, 52 neurons $n = 4$ slices), and while being superfused with ACSF containing 50 μM of the diacylglycerol (DAG) analog 1,2-dioctanoyl-*sn*-glycerol (DOG; ■, 29 neurons, $n = 3$ slices). Both treatments attenuated the $[Ca^{2+}]_i$ increase seen in the absence of stimulation. $t = 0$ is ~90 min from time of animal euthanization. *B*: histograms showing the number of PI-labeled NM neurons in each of the groups in *A*. Error bars represent the standard error of the mean in both *A* and *B* and are <10 nM where not seen in *A*.

120 min (◇, 52 neurons, $n = 4$ slices; same data as in Fig. 3*A*). Superfusing 100 nM PMA prevented this increase: NM neuron mean $[Ca^{2+}]_i$ was 122 ± 7 nM at the beginning of experiments and 139 ± 9 nM after 120 min (○, 52 neurons, $n = 4$ slices). Similarly, superfusion of 50 μM DOG prevented the $[Ca^{2+}]_i$ increase seen in unstimulated NM neurons. NM neuron initial mean $[Ca^{2+}]_i$ was 140 ± 11 nM and after 120 min of DOG superfusion was 163 ± 4 nM (■, 29 neurons, $n = 3$ slices). Both the PMA and DOG groups were significantly different from the control (unstimulated) group ($F_{(24,144)} = 29.81$, $P = 0.0001$ and $F_{(24,120)} = 25.56$, $P = 0.0001$, respectively) but not from each other ($F_{(24,120)} = 0.70$, $P = 0.8424$). Superfusion of the inactive phorbol ester, 4-α-PMA, had no effect on the NM neuron $[Ca^{2+}]_i$ increase (26 neurons, $n = 2$ slices; data not shown).

Figure 5*B* shows that superfusion of PMA or DOG did not have a significant effect on the number of PI-labeled NM neurons ($F_{(5,13)} = 1.89$, $P = 0.1647$).

Figure 6*A* shows that inhibition of PKC with 50 nM bisindolymaleimide partially interrupts 5-Hz stimulation from maintaining NM neuron $[Ca^{2+}]_i$ at physiological levels. Orthodromic stimulation maintained NM neuron $[Ca^{2+}]_i$ at ~100 nM (●, 63 neurons, $n = 5$ slices; same data as in Fig. 4*A*) for 130 min. Application of 50 nM bisindolymaleimide during continuous stimulation resulted in an average NM neuron $[Ca^{2+}]_i$ increase from 117 ± 8 to 171 ± 15 nM after 120 min (□, 43 neurons, $n = 4$ slices), a level significantly higher than during stimulation, but not as high as in the absence of stimulation (see Fig. 5*A*, ◇). In one of the four slices, the nine NM neurons showed a sharp Ca^{2+} spike in response to the onset of bisindolymaleimide superfusion (Fig. 6*A*, *inset*). Two NM neurons peaked at nearly 600 nM, but returned, with six of the remaining seven neurons, to a baseline $[Ca^{2+}]_i$ equivalent to that observed before the application of bisindolymaleimide. One neuron never recovered to <300 nM. The effect of bisindolymaleimide is statistically significant ($F_{(26,182)} = 11.8$, $P = 0.001$).

Inhibition of PLC with 10 μM U73122 resulted in an increase in stimulated NM neuron $[Ca^{2+}]_i$ that increased slightly more rapidly than the increase induced by bisindolymaleimide inhibition of PKC (Fig. 6*A*, ▲, 28 neurons, $n = 3$ slices) but reached the same level at 120 min. NM neuron $[Ca^{2+}]_i$ increased from 141 ± 14 to 182 ± 6 nM at 120 min. Again, this is significantly different from the control stimulated group ($F_{(26,156)} = 4.66$, $P = 0.0001$), but not from the bisindolymaleimide group ($F_{(26,130)} = 0.71$, $P = 0.85$). Application of the inactive control for U73122, U73343 (10 μM), did not affect the ability of 5-Hz stimulation to maintain NM neuron $[Ca^{2+}]_i$ (12 neurons, $n = 2$ slices; data not shown).

Figure 6*B* shows that application of bisindolymaleimide and U73122 did not significantly affect the number of PI-labeled NM neurons ($F_{(5,12)} = 1.873$, $P = 0.1731$), although the numbers again tended to be higher than the control stimulated slices.

These results suggest that PKC activity is involved in, but not solely responsible for, VIIIth nerve activity-dependent NM neuron $[Ca^{2+}]_i$ regulation. The fact that PMA and DOG attenuated the increase in $[Ca^{2+}]_i$ in the absence of stimulation suggests that PKC activity is sufficient to prevent this phenomenon. However, because inhibition of PKC with bisindolymaleimide resulted in an increase that was less than the increase seen in the absence of stimulation, PKC must not be the only factor involved in activity-dependent $[Ca^{2+}]_i$ regulation. One might suggest that the concentration of bisindolymaleimide used did not fully inhibit PKC activity. Bisindolymaleimide is reported to have an IC_{50} of 5 nM (Toullec et al. 1991). Our use of a concentration that is an order of magnitude greater than the reported IC_{50} should ensure complete block of PKC activity.

The observation that the $[Ca^{2+}]_i$ increase in the presence of U73122 was more rapid than in the presence of bisindolymaleimide suggests that the IP_3 branch of the PLC pathway also is involved in VIIIth nerve activity-dependent regulation of NM neuron $[Ca^{2+}]_i$, perhaps through a Ca^{2+}-dependent mechanism such as Ca^{2+}/calmodulin-dependent kinase.

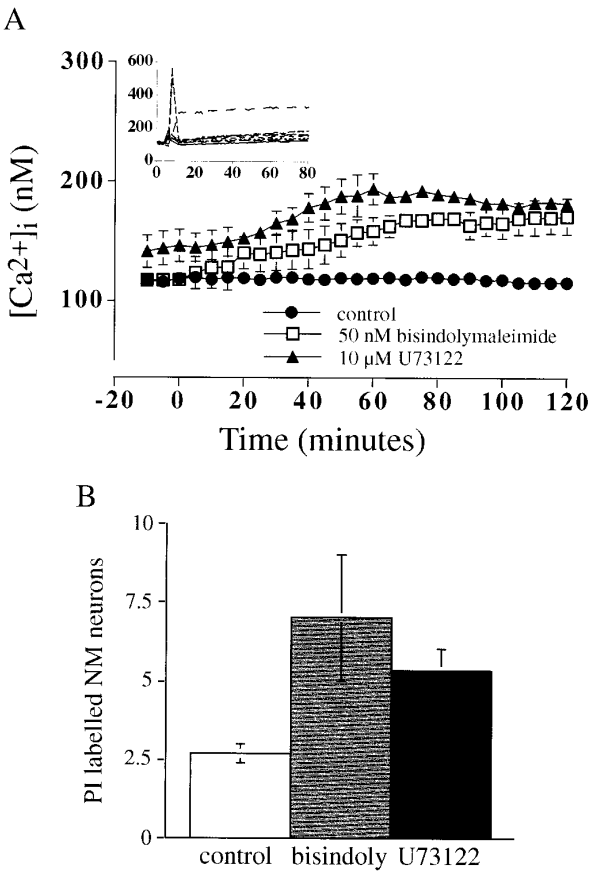

FIG. 6. Inhibition of PKC activity interrupts the ability of continuous orthodromic stimulation to maintain stable NM neuron $[Ca^{2+}]_i$. *A*: mean NM neuron $[Ca^{2+}]_i$ during continuous 5-Hz orthodromic stimulation under the following conditions: control, ACSF only (●, 63 neurons, $n = 5$ slices; same data as in Fig. 4*A*); ACSF containing 50 nM bisindolymaleimide (□, 43 neurons, $n = 4$ slices), and ACSF containing 10 μM U73122 (▲, 28 neurons, $n = 3$ slices). Note that the superfusion of the phospholipase C (PLC) inhibitor U73122 resulted in an $[Ca^{2+}]_i$ increase that was more rapid than that seen with PKC inhibition. *Inset*: $[Ca^{2+}]_i$ traces from 9 NM neurons that received application of bisindolymaleimide at $t = 2$ min during continuous stimulation. Note the sharp "Ca^{2+} spike" occurring at the onset of bisindolymaleimide superfusion. All but 1 cell recovered to normal baseline $[Ca^{2+}]_i$ levels from this response. $t = 0$ is ~90 min from time of animal euthanization. *B*: histograms showing that bisindolymaleimide and U73122 application had no effect on the number of PI-labeled NM neurons. Error bars represent standard error of the mean in both *A* and *B* and are <10 nM where not seen in *A*.

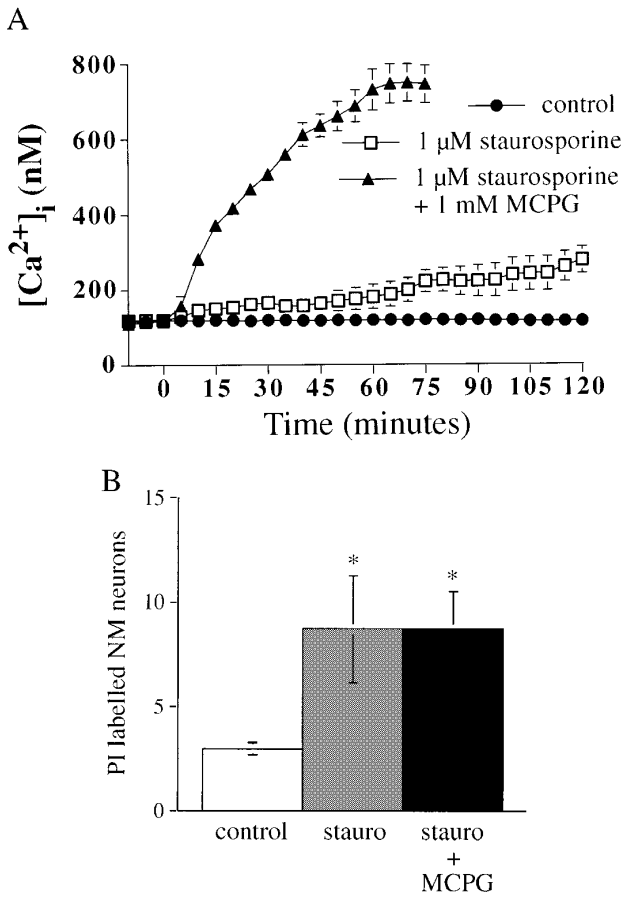

FIG. 7. Effect of kinase and mGluR inhibition on VIIIth nerve activity-dependent NM neuron $[Ca^{2+}]_i$ regulation. *A*: average NM $[Ca^{2+}]_i$ levels are plotted at 5-min intervals in response to three different conditions, all receiving 5-Hz orthodromic stimulation: ●, superfusion of ACSF only (63 neurons, $n = 5$ slices; same data as in Figs. 4*A* and 6*A*); □, superfusion of ACSF containing 1 μM of the nonspecific kinase inhibitor staurosporine at $t = 0$ (32 neurons, $n = 4$ slices), and superfusion of 1 μM staurosporine *and* 1 mM of the nonspecific mGluR antagonist (R,S)-α-methyl-4-carboxyphenylglycine (MCPG) at $t = 0$ (▲, 26 neurons, $n = 3$ slices). Note that the combination of staurosporine and MCPG results in an $[Ca^{2+}]_i$ increase that is greater than staurosporine alone. Error bars represent the standard error of the mean and are <10 nM where not seen. $t = 0$ is ~90 min from time of animal euthanization. *B*: histograms showing the number of PI-labeled NM neurons in each of the experimental groups in *A*. Error bars represent standard error of the mean. *$P < 0.05$ Fisher's protected least significant difference test.

mGluRs, kinases, and NM neuron $[Ca^{2+}]_i$ regulation

The results reported above indicate that PKA and PKC are involved in VIIIth nerve activity-dependent regulation of NM neuron $[Ca^{2+}]_i$. But because inhibition of PKA or PKC never produced an $[Ca^{2+}]_i$ elevation that equaled that observed in the absence of stimulation, other mechanisms must be involved. To test the hypothesis that other kinases are involved, slices were superfused with 1 μM staurosporine, a nonspecific kinase inhibitor, while receiving 5-Hz stimulation. Figure 7*A* shows that 5-Hz stimulation maintains NM neuron $[Ca^{2+}]_i$ at physiological levels (~100 nM) for 130 min (●, 63 neurons $n = 5$ slices, same data as in Figs. 4*A* and 6*A*). Staurosporine application resulted in a gradual increase in NM neuron $[Ca^{2+}]_i$ that reached a concentration of 278 ± 36 nM by 120 min (□, 33 NM neurons, $n = 4$ slices). This was similar in time course and reached a similar amplitude as the increase seen in the absence of stimulation (Figs. 3*A* and 5*A*, ◇) (Zirpel and Rubel 1996a). This effect is significantly different from the stimulated control group ($F_{(26,182)} = 10.46$, $P = 0.0001$), but *not* from the unstimulated control group ($F_{(24,144)} = 1.32$, $P = 0.1759$).

To test the hypothesis that VIIIth nerve activity-dependent regulation of NM neuron $[Ca^{2+}]_i$ is mediated entirely through mGluR stimulation of kinase activity, slices receiving 5-Hz stimulation were superfused with staurosporine and 1 mM MCPG. If the mGluR-dependent $[Ca^{2+}]_i$ regulation is mediated only by staurosporine-sensitive protein kinases, the addition of MCPG to the staurosporine superfusate should result in an identical $[Ca^{2+}]_i$ change as that seen with staurosporine alone. On the other hand, if the mGluR-mediated $[Ca^{2+}]_i$ regulation involves other kinases and/or mechanisms, addition of MCPG should result in an even larger $[Ca^{2+}]_i$ increase than that observed with staurosporine alone. Figure 7*A* shows that NM neuron $[Ca^{2+}]_i$ increased much more rapidly and to a higher amplitude in the presence of staurosporine and MCPG (▲, 26 neurons, $n = 3$ slices) than in the presence of staurosporine alone; 731 ± 55 nM for staurosporine + MCPG versus 181 ± 32 nM for staurosporine alone at 60 min ($F_{(17,85)} = 50.86$, $P = 0.0001$). Zirpel and Rubel (1996a) previously reported that application of 1 mM MCPG to a slice receiving 5-Hz orthodromic stimulation resulted in an increase in $[Ca^{2+}]_i$ that reached a concentration of >550 nM after 55 min: an increase identical in time course and magnitude to that observed in this study on application of MCPG and staurosporine. This indicates that MCPG antagonism of mGluRs is affecting some mechanism of Ca^{2+} regulation other than staurosporine-sensitive kinases and that PKA and PKC have relatively minor but significant contributions to the overall VIIIth nerve activity-dependent $[Ca^{2+}]_i$ regulation in NM neurons.

Slices receiving 5-Hz stimulation that were superfused with staurosporine or staurosporine and MCPG also showed significantly more PI-labeled NM neurons than control slices receiving 5-Hz stimulation while being superfused with ACSF alone (Fig. 7*B*). Control slices stimulated at 5 Hz exhibited an average of 2.67 ± 0.3 (9%) PI-labeled NM neurons. Stimulated slices treated with staurosporine showed an average of 8.67 ± 2.6 (29%) PI-labeled NM neurons, whereas stimulated slices treated with staurosporine and MCPG showed an average of 8.67 ± 1.8 (29%) PI-labeled NM neurons (Fisher's PLSD test, $P = 0.0341$ for both groups). While the latter two groups showed identical increases in the number of PI-labeled cells, it is interesting to note the large differences between them in final $[Ca^{2+}]_i$ levels. This variability is discussed further later.

To confirm the results of the PI incorporation, total number of fura-2–labeled NM neurons were counted at the beginning and end of each of the staurosporine and staurosporine plus MCPG experiments. Complete loss of fura-2 fluorescence is reported to indicate cell death (Johnson et al. 1994). Staurosporine-treated slices showed a 33.5 ± 3.3% decrease in number of fura-2–labeled cells, whereas staurosporine plus MCPG-treated slices showed a 33.0 ± 3.0% decrease. Control, stimulated slices showed only a 13.2 ± 2.7% decrease in fura-2–labeled NM neurons. These results confirm and parallel those obtained with PI incorporation.

DISCUSSION

In this study we have shown that inhibition of PKC, inhibition of PLC, or inhibition of PKA disrupts the ability of VIIIth nerve activity to maintain NM neuron $[Ca^{2+}]_i$ homeostasis, resulting in elevated $[Ca^{2+}]_i$. Additionally, we have shown that nonspecific kinase inhibition also disrupts VIIIth nerve activity-dependent regulation of NM neuron $[Ca^{2+}]_i$ to an extent greater than that of PLC, PKC, or PKA inhibition but equal to that of deafferentation and less than that of mGluR inhibition. Conversely, activation of PKC, adenylate cyclase, or PKA all result in an attenuation of the NM neuron $[Ca^{2+}]_i$ increase normally seen in the absence of stimulation. Finally, the results suggest that increases in $[Ca^{2+}]_i$ are not linearly related to increased cell death at the time points we have investigated but that there appears to be a threshold concentration (250 nM) above which there is a direct relationship between increased $[Ca^{2+}]_i$ and this marker of cell death. In the remainder of this report, we will discuss these results in the context of metabotropic receptors, PKA, and PKC in $[Ca^{2+}]_i$ homeostasis and the relationship between $[Ca^{2+}]_i$ homeostasis and cell death and then examine the functional significance of these data with regard to afferent regulation of NM neurons.

mGluRs, PKA, PKC, and $[Ca^{2+}]_i$ homeostasis

Metabotropic glutamate receptors are well characterized as being linked to the PLC and adenylate cyclase signal transduction cascades (Bockaert et al. 1993; Duvoisin et al. 1995; Nakajima et al. 1993; Okamoto et al. 1994; Schoepp 1993; Tanabe et al. 1992). Previous studies from our lab have shown that NM neurons express one or more mGluR(s) linked to these signal transduction systems and are directly and indirectly involved in $[Ca^{2+}]_i$ homeostasis. Kinases are known to play major roles in neuronal regulation of $[Ca^{2+}]_i$ (Carafoli 1987; Ghosh and Greenberg 1995) and, specifically, PKA and PKC have been shown to phosphorylate and modulate the activities of a number of the component proteins in the $[Ca^{2+}]_i$ homeostatic machinery, including Ca^{2+} ATPases (Carafoli. 1991), IP_3 receptors (Ferris et al. 1991; Taylor and Marshall 1992; Volpe and Alderson-Lang 1990), Ca^{2+}-permeable ionotropic receptors (Glaum and Miller 1993; Kelso et al. 1992; Kinney and Slater 1993; Wang et al. 1991), and voltage-operated Ca^{2+} channels (Haak et al. 1997; Swartz 1993; Zong and Lux 1994). It is therefore not surprising that inhibition of PKC or PKA disrupts VIIIth nerve activity-dependent $[Ca^{2+}]_i$ regulation in NM neurons. However, the observation that activation of PKA or PKC attenuates, but does not entirely prevent, the $[Ca^{2+}]_i$ increase normally seen in the absence of stimulation underscores the notion that NM neuron $[Ca^{2+}]_i$ homeostasis is a complex symphony of a number of various components, which include, but are clearly not limited to, PKA and PKC. This is further supported by the fact that staurosporine application resulted in a larger $[Ca^{2+}]_i$ increase during stimulation than did specific inhibition of either PKA or PKC. At the concentration used, staurosporine is a nonspecific kinase inhibitor (Shapiro et al. 1996) with effects on PKA, PKC, phosphorylase kinase, S6 kinase, $pp60^{v\text{-}src}$, and tyrosine kinases (Hidaka and Kobayashi 1992), suggesting that other kinases are involved in NM neuron $[Ca^{2+}]_i$ homeostasis. Clearly, the role of additional kinases in VIIIth nerve activity-dependent mGluR-mediated NM neuron $[Ca^{2+}]_i$ homeostasis needs to be more thoroughly investigated.

The increase in $[Ca^{2+}]_i$ produced by inhibition of mGluRs with MCPG is much larger than that seen with specific inhibition of either PKC or PKA and even larger than that seen with nonspecific kinase inhibition by staurosporine. This result suggests that mGluRs have a powerful effect on $[Ca^{2+}]_i$ homeostasis, which includes PKA and PKC, but may not be completely inactivated in the absence of VIIIth nerve afferent stimulation. Inhibition of mGluRs during stimulation would affect mGluR-dependent $[Ca^{2+}]_i$ modulatory mechanisms, such as inhibition of influx through ionotropic receptors (Zirpel et al. 1997) and voltage-gated channels (Lachica et al. 1995) and release from stores (Kato et al. 1996), while leaving intact the effects of ionotropic receptor activation; most notably, influx of Ca^{2+} and activation of voltage-gated Ca^{2+} channels. So not only are the $[Ca^{2+}]_i$ dampening effects of mGluRs inhibited, but the mechanisms of increasing $[Ca^{2+}]_i$ still are being activated, thus resulting in the large and rapid increase in $[Ca^{2+}]_i$.

$[Ca^{2+}]_i$ homeostasis and cell death

Perturbation of a cell's $[Ca^{2+}]_i$ homeostasis, or ''set-point,'' can be a lethal insult (Carafoli 1987; Cheng et al. 1994; Ghosh and Greenberg 1995; Larmet et al. 1992; Siesjö 1989). The most well-studied examples are increased $[Ca^{2+}]_i$ associated with excitotoxicity, anoxia, ischemia, seizures (reviewed in Choi 1992), and apoptosis (McConkey et al. 1989; Wyllie et al. 1984). In some situations, this pathway to cell death can be prevented by PKA or PKC activation (Galli et al. 1995; Kaiser and Lipton 1990; Lucas et al. 1994; Maiese et al. 1996; Wakade et al. 1988). We know from previous studies on NM that after deafferentation, NM neurons show elevated $[Ca^{2+}]_i$ (Zirpel et al. 1995a) and that ≈30% of NM neurons will die (Born and Rubel 1985). The propidium iodide results presented in the current report indicate that this relationship is a direct, but not linear, one. Perturbations in NM neuron $[Ca^{2+}]_i$ homeostasis that result in increased $[Ca^{2+}]_i$, such as inhibition of PKA or PKC during stimulation, do not necessarily result in increased cell death (as measured by PI incorporation). However, perturbations in NM neuron $[Ca^{2+}]_i$ homeostasis that result in $[Ca^{2+}]_i$ increases that reach ≥250 nM, such as in vivo cochlea removal or mGluR antagonism with MCPG, consistently result in increased cell death (see Fig. 8).

The data in this figure suggest that there is a ''threshold'' $[Ca^{2+}]_i$ above which some neurons cannot compensate or recover and eventually die. This idea is further supported by the Fig. 6, *inset*: NM neurons treated with bisindolymaleimide showed a rapid Ca^{2+} spike that peaked >500 nM. All but one of the neurons recovered from this challenge, and baseline $[Ca^{2+}]_i$ levels returned to normal (≈100 nM). The single neuron that did not recover showed $[Ca^{2+}]_i$ that remained >300 nM for the duration of the experiment. This neuron is presumably one of the few in that slice that were dying or dead and thus labeled with PI. Single cell correlations between $[Ca^{2+}]_i$ and PI labeling were not performed, but population analyses support this hypothesis. Alternatively, the Ca^{2+}-induced cell death process may proceed at

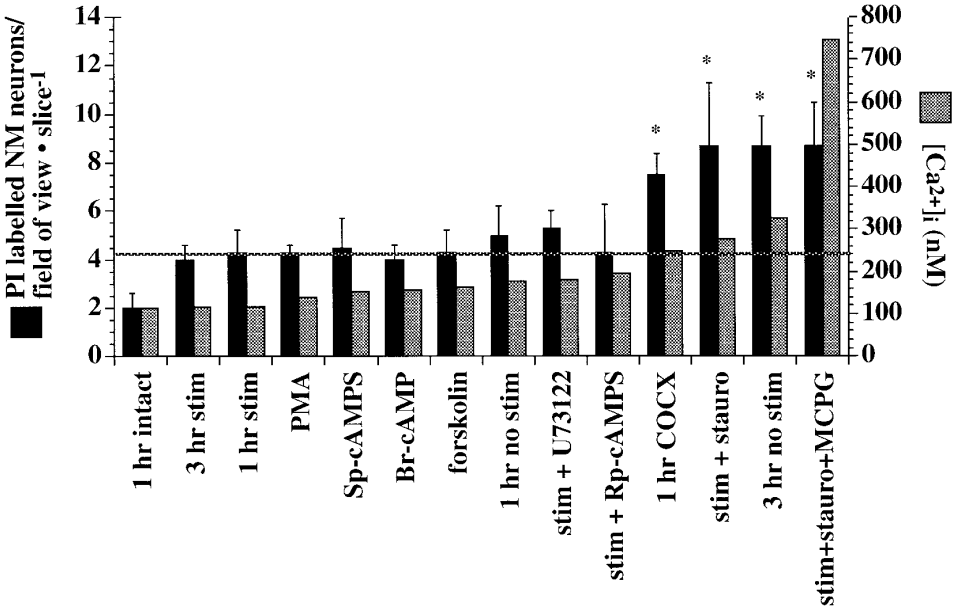

FIG. 8. Treatments that result in an increase in NM neuron $[Ca^{2+}]_i \geq 250$ nM also result in an increase in PI labeling. Histograms showing the peak $[Ca^{2+}]_i$ of each of the treatments presented in this report and the corresponding number of PI-labeled NM neurons in the same group. Note that the only conditions that result in an increase in number of PI-labeled NM neurons (when compared with appropriate controls; see earlier sections) are those that produce an increase in $[Ca^{2+}]_i > 250$ nM. Error bars represent standard error of the mean.

a slower rate for the smaller $[Ca^{2+}]_i$ increases and does not appear at the time points observed in this study.

There were two surprising features of these results. The first is the rapidity with which NM neurons incorporated PI after loss of orthodromic stimulation. Despite the fact that $[Ca^{2+}]_i$ is elevated to $\approx$ 250 nM 1 h after an in vivo cochlea removal, it was unexpected that the NM neurons would show PI incorporation so soon. Previous studies have shown that all NM neuron cell bodies are present 24 h after a cochlea removal and that cell counts are not significantly different between intact and deafferented sides until 24–48 h (Born and Rubel 1985). However, within 30 min of deafferentation, NM neurons show decreases in protein synthesis that continue for another 11.5 h. At 12 h, NM shows two distinct population of cells: those that have reduced protein synthesis and presumably will survive and those that are devoid of ribosomes and protein synthesis and presumably will die (Garden et al. 1994; Steward and Rubel 1985). Four hours after insult, cells undergoing induced apoptosis show an increase in DNA fragmentation that disappears after 24 h (Li et al. 1996). A hallmark of apoptosis is DNA degradation by Ca^{2+}-dependent endonucleases (Cohen and Duke 1984; Wyllie et al. 1984). A similar course of events may be occurring in NM with PI labeling. The neurons that label with PI at early time points may still be alive and functioning but are already undergoing degenerative changes (e.g., DNA degradation by Ca^{2+}-dependent endonucleases) that will result in their eventual death.

PI staining is a membrane-delimited process and is thus a direct measure of membrane integrity (Bevensee et al. 1995; Dengler et al. 1995; Lizard et al. 1995). A leaky membrane is one of the *early* signals of a cell in a pathological state and is the principle on which exclusion dyes and ''live-cell'' fluorescent markers are based (Gray and Morris 1987; Kolber et al. 1988; Nicoletti et al. 1991; Suzuki et al. 1991). PI labeling occurs before DNA fragmentation in apoptotic cells (Lizard et al. 1995) and has been shown to label *dying* cells in excitotoxic (Wilde et al. 1994), hypercalcemic (Jiang et al. 1993; Kuroda et al. 1995), and necrotic conditions (Lizard et al. 1995). PI labeling also correlates well with other cell death assays such as fluorescent live-cell markers (Bevensee et al. 1995; Johnson et al. 1994), trypan blue exclusion (Behl et al. 1995), and lactate dehydrogenase release (Bruce et al. 1995; Jiang et al. 1993; Vornov et al. 1991). This instills confidence that PI-labeled NM neurons are indeed either dead or in the process of dying. However, these data give no indication as to the cause of the cell death process (viz hypercalcemia). PI also has been shown to label other cell types in parallel with changes $[Ca^{2+}]_i$ and intracellular pH (Bevensee et al. 1995; Kuroda et al. 1995), all of which are likely due to a leaky plasma membrane. It is accepted that excitotoxic cell death is dependent on increased $[Ca^{2+}]_i$ (reviewed in Choi 1992), but the contribution of increased $[Ca^{2+}]_i$ to other forms of apoptosis is controversial (reviewed in Lee et al. 1993). We are therefore cautious in stating that PI labeling *corresponds* with increases in NM neuron $[Ca^{2+}]_i > 250$ nM under conditions that are known to result in increased NM neuron death. Experiments are being conducted to determine the direct relationship between increased $[Ca^{2+}]_i$ and PI labeling in deafferentation-induced NM neuron death.

The second surprising result of the PI labeling experiments reported here is the relatively low threshold of $[Ca^{2+}]_i$ that results in cell death. Although there is not a single intracellular calcium concentration deemed pathological or lethal, most insults resulting in cell death produce on the order of 10-fold increases in baseline $[Ca^{2+}]_i$ (e.g., Tymianski et al. 1993). However, many of these paradigms produce large, *transient* increases that may trigger, but are not directly related to, the subsequent, gradual $[Ca^{2+}]_i$ increase that results in cell death. Choi (1985) demonstrated that excitotoxicity is a biphasic process in which a delayed type of cellular damage, with overt cell destruction, was dependent on Ca^{2+} influx. Similarly, Rothman and Olney (1986) concluded that in hypoxia-ischemia, excitatory amino acids cause two types of neuronal damage: an initial osmolytic type and a delayed calcium-dependent type. This biphasic mechanism of Ca^{2+}-dependent cell degeneration and death has been replicated in a number of systems and has become accepted widely as a common mechanism of cell death involving glutamate

(Manev et al. 1989; Randall and Thayer 1992; reviewed in Choi 1992; Rothman 1992). Other studies have shown that $[Ca^{2+}]_i$ increases of hundreds of nanomolar can result in cell death in cultured hippocampal neurons (Michaels and Rothman 1990; Randall and Thayer 1992). Therefore, in NM neurons, the $[Ca^{2+}]_i$ increases that we have characterized may be sufficient to cause degeneration and death, if indeed Ca^{2+} is the causative agent.

Functional significance

Survival, morphology, physiology, and metabolism of developing CNS neurons are all dependent on afferent sensory input (Brunjes 1994; Dubin et al. 1986; Globus 1975; Hubel and Wiesel 1970; Moore 1992; Wiesel and Hubel 1963a,b; Woolf et al. 1983). Although these phenomena are well characterized in every sensory system, the inter- and intracellular cascades responsible for changes in neuronal composition are not well understood. In our quest to elucidate these mechanisms in the developing auditory system of the chick, we have shown that NM neuron's dependence on VIIIth nerve activity is mediated by mGluRs that transduce the glutamatergic signal from the VIIIth nerve terminals into the intracellular messengers IP_3, Ca^{2+}, and cAMP (reviewed in Zirpel et al. 1997). The present report elucidates further the roles of the effector enzymes of these messengers, specifically PKA and PKC, in regulating intracellular calcium, and relates $[Ca^{2+}]_i$ increases with cell death. The following hypothesis of VIIIth nerve activity-dependent mGluR-mediated maintenance of NM neurons is based on this and previous studies from these laboratories and is the foundation for ongoing and future studies.

During normal VIIIth nerve activity, iGluRs and mGluRs on NM neurons are activated. Activation of the iGluRs results in a depolarizing electrical response in the postsynaptic NM neurons that is carried in part by an influx of Ca^{2+} ions (Otis et al. 1995; Zhou et al. 1995). This depolarization opens L-type Ca^{2+} channels that allow influx of Ca^{2+}. Activation of mGluRs results in stimulation of phospholipase C producing IP_3 (Zirpel et al. 1994) and DAG and stimulation of adenylate cyclase producing cAMP (Lachica et al. 1995). IP_3 releases Ca^{2+} from intracellular stores (Zirpel et al. 1995b) that subsequently binds to calmodulin (CaM) and activates Ca^{2+}/CaM-dependent kinase (CaM kinase). DAG together with the calcium released by IP_3 activates PKC (Nishizuka 1986). To ensure a proper Ca^{2+} signal to activate CaM kinase and PKC, a calcium-induced calcium-release (CICR) mechanism also is activated (Kato et al. 1996). The cAMP activates PKA, which then phosphorylates and negatively modulates L-type Ca^{2+} channels, Ca^{2+}-permeable iGluRs, and CICR mechanisms (reviewed in Zirpel et al. 1997). The activated CaM kinase and PKC also phosphorylate their various substrates, which serve as $[Ca^{2+}]_i$-decreasing mechanisms, such as speeding up Ca^{2+} ATPases, and negatively modulating Ca^{2+} increasing mechanisms such as voltage-operated Ca^{2+} channels, *N*-methyl-D-aspartate (NMDA) receptors and Ca^{2+} permeable iGluRs (Bleakman et al. 1992; Ferris et al. 1991; Hawkins et al. 1995; Mayrleitner et al. 1995; Miller 1986; Stoclet et al. 1987). NM neuron $[Ca^{2+}]_i$ homeostasis during normal VIIIth nerve activity is a balance between these Ca^{2+}-increasing and -decreasing processes, which reach equilibrium at ≈100 nM (Zirpel and Rubel 1996a). It also must be kept in mind that none of these signal transduction systems functions linearly or independently; each modulates another, and there are modulatory feedback mechanisms for each step in a given pathway (Hille 1992). For example, Ca^{2+} plays a negative modulatory role in release from stores (Suppatone et al. 1988; Taylor and Marshall 1992) and influx through NMDA-receptor channels (Legendre et al. 1993; Vyklicky 1993). On deafferentation, the mGluR-mediated negative modulation of the Ca^{2+}-increasing processes is no longer present, and the balance is shifted toward an increase in $[Ca^{2+}]_i$ by spontaneous release from stores (Missiaen et al. 1991), influx leak, and/or spontaneous and driven activity from the contralateral superior olive projection (Westerberg and Schwarz 1995). Increased $[Ca^{2+}]_i$ then activates Ca^{2+}-dependent endonucleases and proteases and sets in motion the cell degeneration process. Twenty to 40% of the NM neurons cannot cope with this hypercalcemia and eventually die. The remaining NM neurons can implement compensatory mechanisms, such as increased mitochondrial function (Hyde and Durham 1994a,b), that allow them to survive. Many pieces of this picture are still unclear, but the hypotheses are consistent with the current and previous data on NM neurons and signal transduction pathways.

Why might NM neurons express such a strong mGluR-mediated modulation of Ca^{2+}? NM neurons phase-lock to frequencies ≤9,000 Hz and show spontaneous rates of 100 Hz (Warchol and Dallos 1990). NM neurons also are enveloped by specialized calyceal terminals (Carr and Boudreau 1991; Parks and Rubel 1978), the end-bulbs of Held, that cover approximately two-thirds of the neuron's surface (Parks 1981). Glutamate may exceed millimolar concentrations within the synaptic cleft (Clements 1996) that can persist for milliseconds (Clements 1996; Jonas and Spruston 1994). Prolonged exposure of 66% of a neuron's surface to that high of a concentration of glutamate places NM neurons in a potentially excitotoxic environment. The implementation of a mechanism to keep Ca^{2+} increases in check would provide a beneficial survival strategy for NM neurons. Hence, mGluRs may serve a very important neuroprotective function for NM neurons during normal VIIIth nerve neurotransmission.

We thank J. Shang for performing excellent dissections and general technical assistance, to G. H. MacDonald for assistance with the Bio-Rad MRC 1024, National Institutes of Health Image, and image processing, and M. Russo for clerical and editorial assistance.

This work was supported by National Institute of Deafness and Other Communications Disorders Grants DC-00520 and DC-00774.

Present address of L. Zirpel: Dept. of Neurobiology and Anatomy, University of Utah School of Medicine, 50 N. Medical Dr., Salt Lake City, UT 84132.

Address reprint requests to E. W Rubel.

Received 22 October 1997; accepted in final form 16 December 1997.

REFERENCES

BEHL, C., WIDMANN, M., TRAPP, T., AND HOLSBOER, F. 17-beta estradiol protects neurons from oxidative stress-induced cell death in vitro. *Biochem. Biophys. Res. Commun.* 216: 473–482, 1995.

BEVENSEE, M. O., SCHWIENING, C. J., AND BORON, W. F. Use of BCECF and propidium iodide to assess membrane integrity of acutely isolated CA1 neurons from rat hippocampus. *J. Neurosci. Methods* 58: 61–75, 1995.

BLEAKMAN, D., RUSIN, K. I., CHARD, P. S., GLAUM, S. R., AND MILLER,

R. J. Metabotropic glutamate receptors potentiate ionotropic glutamate responses in the rat dorsal horn. *Mol. Pharmacol.* 42: 192–196, 1992.

BOCKAERT, J., PIN, J., AND FAGNI, L. Metabotropic glutamate receptors: an original family of G protein-coupled receptors. *Fundam. Clin. Pharmacol.* 7: 473–485, 1993.

BORN, D. E., DURHAM, D., AND RUBEL, E. W Afferent influences on brainstem auditory nuclei of the chick: nucleus magnocellularis neuronal activity following cochlea removal. *Brain Res.* 557: 37–47, 1991.

BORN, D. E. AND RUBEL, E. W Afferent influences on brain stem auditory nuclei of the chicken: neuron number and size following cochlea removal. *J. Comp. Neurol.* 231: 435–445, 1985.

BRUCE, A. J., SAKHI, S., SCHREIBER, S. S., AND BAUDRY, M. Development of kainic acid and *N*-methyl-D-aspartic acid toxicity in organotypic hippocampal cultures. *Exp. Neurol.* 132: 209–219, 1995.

BRUNJES, P. C. Unilateral naris closure and olfactory system development. *Brain Res. Rev.* 19: 146–160, 1994.

CARAFOLI, E. Intracellular calcium homeostasis. *Annu. Rev. Biochem.* 56: 395–433, 1987.

CARR, C. E. AND BOUDREAU, R. E. Central projections of auditory nerve fibers in the barn owl. *J. Comp. Neurol.* 314: 306–318, 1991.

CHENG, B., CHRISTAKOS, S., AND MATTSON, M. P. Tumor necrosis factors protect neurons against metabolic-excitotoxic insults and promote maintenance of calcium homeostasis. *Neuron.* 12: 139–153, 1994.

CHOI, D. W. Glutamate neurotoxicity in cortical cell culture is calcium dependent. *Neurosci. Lett.* 58: 293–297, 1985.

CHOI, D. W. Excitotoxic cell death. *J. Neurobiol.* 23: 1261–1276, 1992.

CLEMENTS, J. D. Transmitter timecourse in the synaptic cleft: its role in central synaptic function. *Trends Neurosci.* 19: 163–171, 1996.

COHEN, J. J. AND DUKE, R. C. Glucocorticoid activation of a calcium-dependent endonuclease in thymocyte nuclei leads to cell death. *J. Immunol.* 132: 38–42, 1984.

COLLINS, F., SCHMIDT, M. F., GUTHRIE, P. B., AND KATER, S. B. Sustained increase in intracellular calcium promotes neuronal survival. *J. Neurosci.* 11: 2582–2587, 1991.

DENGLER, W. A., SCHULTE, J., BERGER, D. P., MERTELSMANN, R., AND FIEBIG, H. H. Development of a propidium iodide fluorescence assay for proliferation and cytotoxicity assays. *Anticancer Drugs* 6: 522–532, 1995.

DUBIN, M. W., STARK, L. A., AND ARCHER, S. M. A role for action-potential activity in the development of neuronal connections in the kitten retinogeniculate pathway. *J. Neurosci.* 6: 1021–1036, 1986.

DUVOISIN, R. M., ZHANG, C., AND RAMONELL, K. A novel metabotropic glutamate receptor expressed in the retina and olfactory bulb. *J. Neurosci.* 15: 3075–3083, 1995.

ELKABES, S., CHERRY, J. A., SCHOUPS, A. A., AND BLACK, I. B. Regulation of protein kinase C activity by sensory deprivation in the olfactory and visual systems. *J. Neurochem.* 60: 1835–1842, 1993.

ERAUSQUIN, G.A.D., MANEV, H., GUIDOTTI, A., COSTA, E., AND BROOKER, G. Gangliosides normalize distorted single-cell intracellular free Ca^{2+} dynamics after toxic doses of glutamate in cerebellar granule cells. *Proc. Natl. Acad. Sci. USA* 87: 8017–8021, 1990.

FERRIS, C. D., HUGANIR, R. L., BREDT, D. S., CAMERON, A. M., AND SNYDER, S. H. Inositol trisphosphate receptor: phosphorylation by protein kinase C and calcium calmodulin-dependent protein kinases in reconstituted lipid vesicles. *Proc. Natl. Acad. Sci. USA* 88: 2232–2235, 1991.

FRANKLIN, J. L., JOHNSON, E. M., JR. Suppression of programmed neuronal death by sustained elevation of cytoplasmic calcium. *Trends Neurosci.* 15: 501–508, 1992.

FUKAYAMA, S., TASHJIAN, A. H., JR., AND BRINGHURST, F. R. Role of protein kinase A in the regulation of cytosolic free calcium in human osteoblast-like SaOS-2 cells. *Am. J. Physiol.* 264 (*Cell. Physiol.*33): C464–C470, 1993.

FURUKAWA, K., MATTSON, M. P. Cytochalasins protect hippocampal neurons against amyloid β-peptide toxicity: evidence that actin depolymerization suppresses Ca^{2+} influx. *J. Neurochem.* 65: 1061–1068, 1995.

GALLI, C., MEUCCI, O., SCORZIELLO, A., WERGE, T. M., CALISSANO, P., AND SCHETTINI, G. Apoptosis in cerebellar granule cells is blocked by high KCl, forskolin, and IGF-1 through distinct mechanisms of action: the involvement of intracellular calcium and RNA synthesis. *J. Neurosci.* 15: 1172–1179, 1995.

GARDEN, G. A., CANADY, K. S., LURIE, D. I., BOTHWELL, M., AND RUBEL, E. W A biphasic change in ribosomal conformation during transneuronal degeneration is altered by inhibition of mitochondrial, but not cytoplasmic protein synthesis. *J. Neurosci.* 14: 1994–2008, 1994.

GHOSH, A. AND GREENBERG, M. E. Calcium signalling in neurons: molecular mechanisms and cellular consequences. *Science* 268: 239–247, 1995.

GLAUM, S. R. AND MILLER, R. J. Activation of metabotropic glutamate receptors produces reciprocal regulation of ionotropic glutamate and GABA responses in the nucleus of the tractus solitarius of the rat. *J. Neurosci.* 13: 1636–1641, 1993.

GLOBUS, A. Brain morphology as a function of presynaptic morphology and activity. In: *The Developmental Neuropsychology of Sensory Deprivation.* New York: Academic Press, 1975, p. 9–91.

GRAY, D.W.R. AND MORRIS, P. J. The use of fluoroscein diacetate and ethidium bromide as a viability stain for isolated Islets of Langerhans. *Stain Technol.* 62: 373–382, 1987.

GREENGARD, P., JEN, J., NAIRN, A. C., AND STEVENS, C. F. Enhancement of the glutamate response by cAMP-dependent protein kinase in hippocampal neurons. *Science* 253: 1135–1138, 1991.

GRIERSON, J. P. AND MELDOLESI, J. Calcium homeostasis in mouse fibroblast cells: affected by U-73122, a putative phospholipase Cβ blocker, via multiple mechanisms. *Br. J. Pharmacol.* 115: 11–14, 1995.

GRYNKIEWICZ, G., POENIE, M., AND TSIEN, R. Y. A new generation of Ca^{2+} indicators with greatly improved fluorescence properties. *J. Biol. Chem.* 260: 3440–3450, 1985.

HAAK, L. L., HELLER, C., AND VAN DEN POL, A. N. Metabotropic glutamate receptor activation modulates kainate and serotonin calcium response in astrocytes. *J. Neurosci.* 17: 1825–1837, 1997.

HAWKINS, C., XU, A., AND NARAYANAN, N. Comparison of the effects of the membrane-associated Ca^{2+}/calmodulin-dependent kinase on Ca^{2+}-ATPase function in cardiac and slow-twitch skeletal muscle sarcoplasmic reticulum. *Mol. Cell. Biochem.* 142: 131–138, 1995.

HIDAKA, H. AND KOBAYASHI, R. Pharmacology of protein kinase inhibitors. *Annu. Rev. Pharmacol. Toxicol.* 32: 377–397, 1992.

HILLE, B. G protein-coupled mechanisms and nervous signaling. *Neuron* 9: 187–195, 1992.

HUBEL, D. H. AND WIESEL, T. N. The period of susceptibility to the physiological effects of unilateral eye closure in kittens. *J. Physiol. (Lond.)* 206: 419–436, 1970.

HYDE, G. E. AND DURHAM, D. Increased deafferentation-induced cell death in chick brainstem auditory neurons following blockade of mitochondrial protein synthesis with chloramphenicol. *J. Neurosci.* 14: 291–300, 1994a.

HYDE, G. E. AND DURHAM, D. Rapid increase in mitochrondial volume in nucleus magnocellularis neurons following cochlea removal. *J. Comp. Neurol.* 339: 27–48, 1994b.

HYSON, R. L. AND RUBEL, E. W Transneuronal regulation of protein synthesis in the brain stem auditory system of the chick requires synaptic activation. *J. Neurosci.* 9: 2835–2845, 1989.

INCE, C., VAN DISSEL, J. T., AND DIESSELHOFF, M.M.C. A teflon culture dish for high-magnification microscopy and measurements in single cells. *Pflügers Arch.* 403: 240–244, 1985.

JACKSON, H., NEMETH, E. F., AND PARKS, T. N. Non-*N*-methyl-D-aspartate receptors mediating synaptic transmission in the avian cochlear nucleus: effects of kynurenic acid, dipicolinic acid and streptomycin. *Neuroscience* 16: 171–179, 1985.

JIANG, T., GRANT, R. L., AND ACOSTA, D. A digitized fluorescence imaging study of intracellular free calcium, mitochondrial integrity and cytotoxicity in rat renal cells exposed to ionomycin, a calcium ionophore. *Toxicology* 85: 41–65, 1993.

JOHNSON, M. E., GORES, G. J., UHL, C. B., AND SILL, J. C. Cytosolic free calcium and cell death during metabolic inhibition in a neuronal cell line. *J. Neurosci.* 14: 4040–4049, 1994.

JONAS, P. AND SPRUSTON, N. Mechanisms shaping glutamate-mediated excitatory postsynaptic currents in the CNS. *Curr. Opin. Neurobiol.* 4: 366–372, 1994.

KAISER, P. K. AND LIPTON, S. A. VIP-mediated increase in cAMP prevents tetrodotoxin-induced retinal ganglion cell death in vitro. *Neuron* 5: 373–381, 1990.

KATO, B. M., LACHICA, E. A., AND RUBEL, E. W Glutamate modulates intracellular Ca^{2+} stores in brainstem auditory neurons. *J. Neurophysiol.* 76: 646–650, 1996.

KEBABIAN, J. W. The cyclic AMP cascade: a signal transduction system. *Neurotransmissions* 8: 1–4, 1992.

KELSO, S. R., NELSON, T. E., AND LEONARD, J. P. Protein kinase c-mediated enhancement of NMDA currents by metabotropic glutamate receptors in *Xenopus* oocytes. *J. Physiol. (Lond.)* 449: 705–718, 1992.

KENNEDY, M. B. Regulation of neuronal function by calcium. *Trends Neurosci.* 12: 417–419, 1989.

KIKKAWA, U., KITANO, T., SAITO, N., KISHIMOTO, A., TANIYAMA, K., TANAKA, C., AND NISHIZUKA, Y. Role of protein kinase C in calcium-mediated signal transduction. In: *Calcium and the Cell.* Chichester, UK: Wiley, 1986, p. 197–211.

KINNEY, G. A. AND SLATER, N. T. Potentiation of NMDA receptor-mediated transmission in turtle cerebellar granule cells by activation of metabotropic glutamate receptors. *J. Neurophysiol.* 69: 585–594, 1993.

KOIKE, T., MARTIN, D. P., AND JOHNSON, E. M., JR. Role of Ca^{2+} channels in the ability of membrane depolarization to prevent neuronal death induced by trophic-factor deprivation: evidence that levels of internal Ca^{2+} determine nerve growth factor dependence of sympathetic ganglion cells. *Proc. Natl. Acad. Sci. USA* 86: 6421–6425, 1989.

KOLBER, M. A., QUINONES, R. R., GRESS, R. E., HENKART, P. A. Measurement of cytotoxicity by target cell release and retention of the fluorescent dye bis-carboxyethyl-carboxyfluorescein (BCECF). *J. Immunol. Methods* 108: 255–264, 1988.

KURODA, Y., TAKEDA, K., TABEI, K., KUORKI, M., YAGIMUMA, T., OHARA, T., AND ASANO, Y. Role of $[Ca^{2+}]_i$ in lethal oxidative injury in rat cultured inner medullary collecting duct cells. *Pflügers Arch.* 430: 697–704, 1995.

LACHICA, E. A., RÜBSAMEN, R., ZIRPEL, L., AND RUBEL, E. W Glutamatergic inhibition of voltage-operated calcium channels in the avian cochlear nucleus. *J. Neurosci.* 15: 1724–1734, 1995.

LARMET, Y., DOLPHIN, A. C., AND DAVIES, A. M. Intracellular calcium regulates the survival of early sensory neurons before they become dependent on neurotrophic factors. *Neuron* 9: 563–574, 1992.

LEE, S., CHRISTAKOS, S., SMALL, M. B. Apoptosis and signal transduction: clues to a molecular mechanism. *Curr. Opin. Cell. Biol.* 5: 286–291, 1993.

LEGENDRE, P., ROSENMUND, C., AND WESTBROOK, G. L. Inactivation of NMDA channels in cultured hippocampal neurons by intracellular calcium. *J. Neurosci.* 13: 674–684, 1993.

LI, Y. Q., GUO, Y. P., JAY, V., STEWART, P. A., AND WONG, C. S. Time course of radiation-induced apoptosis in the adult rat spinal cord. *Radiother. Oncol.* 39: 35–42, 1996.

LIPPE, W. R. Rhythmic spontaneous activity in the developing avian auditory system. *J. Neurosci.* 14: 1486–1495, 1994.

LIZARD, G., FOURNEL, S., GENESTIER, L., DHEDIN, N., CHAPUT, C., FLACHER, M., MUTIN, M., PANAYE, G., AND REVILLARD, J. P. Kinetics of plasma membrane and mitochondrial alterations in cells undergoing apoptosis. *Cytometry* 21: 275–283, 1995.

LONDON, N. J., CONTRACTOR, H., LAKE, S. P., AUCOTT, G. C., BELL, P. R., AND JAMES, R. F. A microfluorometric viability assay for isolated human and rat islets of Langerhans. *Diabetes Res.* 12: 141–149, 1989.

LUCAS, M., SANCHEZ-MARGALET, V., SANZ, A., AND SOLANO, F. Protein kinase C activation promotes cell survival in mature lymphocytes prone to apoptosis. *Biochem. Pharmacol.* 47: 667–672, 1994.

MADISON, D. V. AND NICOLL, R. A. Cyclic adenosine 3′, 5′-monophosphate mediates B-receptor actions of noradrenaline in rat hippocampal pyramidal cells. *J. Physiol. (Lond.)* 372: 245–259, 1986.

MAIESE, K., SWIRIDUK, M., AND TENBROEKE, M. Cellular mechanisms of protection by metabotropic glutamate receptors during anoxia and nitric oxide toxicity. *J. Neurochem.* 66: 2419–2248, 1996.

MALENKA, R. C., MADISON, D. V., ANDRADE R., AND NICOLL, R. A. Phorbol esters mimic some cholinergic actions in hippocampal pyramidal neurons. *J. Neurosci.* 6: 475–480, 1986.

MANEV, H., FAVARON, M., GUIDOTTI, A., AND COSTA, E. Delayed increase of Ca^{2+} influx elicited by glutamate: role in neuronal death. *Mol. Pharmacol.* 36: 106–112, 1989.

MARTIN, M. Excitatory amino acid pharmacology of the auditory nerve and nucleus magnocellularis of the chicken. *Hear. Res.* 17: 153–160, 1985.

MAYRLEITNER, M., CHANDLER, R., SCHINDLER, H., AND FLEISCHER, S. Phosphorylation with protein kinases modulates calcium loading of terminal cisternae of sarcoplsmic reticulum from skeletal muscle. *Cell. Calcium* 18: 197–206, 1995.

MCCONKEY, D. J., NICOTERA, P., HARTZELL, P., BELLOMO, G., WYLLIE, A. H., AND ORRENIUS, S. Glucocorticoids activate a suicide process in thymocytes through an elevation of cytosolic Ca^{2+} concentration. *Arch. Biochem. Biophys.* 269: 365–370, 1989.

MICHAELS, R. L. AND ROTHMAN, S. M. Glutamate neurotoxicity in vitro: antagonist pharmacology and intracellular calcium concentrations. *J. Neurosci.* 10: 283–292, 1990.

MILLER, R. J. Protein kinase C: a key regulator of neuronal excitability? *Trends Neurosci.* 9: 538–541, 1986.

MILLS, L. R. AND KATER, S. B. Neuron-specific and state-specific differences in calcium homeostasis regulate the generation and degeneration of neuronal architecture. *Neuron* 2: 149–163, 1990.

MISSIAEN, L., TAYLOR, C. W., AND BERRIDGE, M. J. Spontaneous calcium release from inositol trisphosphate sensitive calcium stores. *Nature* 352: 241–244, 1991.

MOORE, D. R. Developmental plasticity of the brainstem and midbrain auditory nuclei. In: *Development of Auditory and Vestibular Systems 2.* Amsterdam, Elsevier, 1992, p. 297–320.

NAKAJIMA, Y., IWAKABE, H., AKAZAWA, C., NAWA, H., SHIGEMOTO, R., MIZUNO, N., AND NAKANISHI S. Molecular characterization of a novel retinal metabotropic glutamate receptor mGluR6 with a high agonist selectivity for L-2-amino-4-phosphonobutyrate. *J. Biol. Chem.* 268: 11868–11873, 1993.

NEMETH, E. F., JACKSON, H., AND PARKS, T. N. Pharmacological evidence for synaptic transmission mediated by non-*N*-methyl-D-aspartate receptors in the avian cochlear nucleus. *Neurosci. Lett.* 40: 39–44, 1983.

NICOLETTI, F., WROBLEWSKI, J. T., ALHO, H., EVA, C., FADDA, E., AND COSTA, E. Lesions of the putative glutamatergic pathways potentiate the increase of inositol phospholipid hydrolysis elicited by excitatory amino acids. *Brain Res.* 436: 103–112, 1987.

NICOLETTI, I., MIGLIORATI, G., PAGLIACCI, M. C., GRIGNANI, F., AND RICCARDI, C. A rapid and simple method for measuring thymocyte apoptosis by propidium iodide staining and flow cytometry. *J. Immunol. Methods* 139: 271–279, 1991.

NISHIZUKA, Y. The role of protein kinase C in cell surface transduction and tumor promotion. *Nature* 308: 691–698, 1984.

NISHIZUKA, Y. Studies and perspectives of protein kinase C. *Science* 233: 305–311, 1986.

OKAMOTO, N., HORI, S., AKAZAWA, C., HAYASHI, Y., SHIGEMOTO, R., MIZUNO, N., AND NAKANISHI S. Molecular cloning of a new metabotropic glutamate receptor mGluR7 coupled to inhibitory cyclic AMP signal transduction. *J. Biol. Chem.* 269: 1231–1236, 1994.

OTIS, T. S., RAMAN, I. M., TRUSSELL, L. O. AMPA receptors with high Ca^{2+} permeability mediate synaptic transmission in the avian auditory pathway. *J. Physiol. (Lond.)* 482: 309–315, 1995.

PARKS, T. N. Changes in the length and organization of nucleus laminaris dendrites after unilateral otocyst ablation in chick embryos. *J Comp Neurol* 202: 47–57, 1981.

PARKS, T. N. AND RUBEL, E. W Organization and development of brain stem auditory nuclei of the chicken: primary afferent projections. *J. Comp. Neurol.* 180: 439–448, 1978.

RAMAN, I. M. AND TRUSSELL, L. O. The kinetics of the response to glutamate and kainate in neurons of the avian cochlear nucleus. *Neuron* 9: 173–186, 1992.

RANDALL, R. D. AND THAYER, S. A. Glutamate-induced calcium transient triggers delayed calcium overload and neurotoxicity in rat hippocampal neurons. *J. Neurosci.* 12: 1881–1895, 1992.

ROTHMAN, S. Excitotoxins: possible mechanisms of action. *Ann. NY Acad. Sci.* 648: 132–139, 1992.

ROTHMAN, S. M. AND OLNEY, J. W. Glutamate and the pathophysiology of hypoxic-ischemic brain damage. *Ann. Neurol.* 19: 105–111, 1986.

RUBEL, E. W, HYSON, R. L., AND DURHAM, D. Afferent regulation of neurons in the brain stem auditory system. *J. Neurobiol.* 21: 169–196, 1990.

SCHOEPP, D. D. The biochemical pharmacology of metabotropic glutamate receptors. *Biochem. Soc. Trans.* 21: 97–102, 1993.

SHAPIRO, M. S., ZHOU, J., AND HILLE, B. Selective disruption by protein kinases of G-protein-mediated Ca^{2+} channel modulation. *J. Neurophysiol.* 76: 311–320, 1996.

SIESJÖ, B. K. Calcium and cell death. *Magnesium* 8: 223–237, 1989.

STEWARD, O. AND RUBEL, E. W Affferent influences on brain stem auditory nuclei of the chicken: Cessation of amino acid incorporation as an antecedent to age-dependent transneuronal degeneration. *J. Comp. Neurol.* 231: 385–395, 1985.

STOCLET, J.-C., GERARD, D., KILHOEFFER, M.-C., LUGNIER, C., MILLER, R., AND SCHAEFFER, P. Calmodulin and its role in calcium regulation. *Prog. Neurobiol.* 29: 321–364, 1987.

SUPPATONE, S., WORLEY, P. F, BARABAN, J. M., AND SNYDER, S. H. Solubilization, purification, and characterization of an inositol trisphosphate receptor. *J. Biol. Chem.* 263: 1530–1534, 1988.

SUZUKI, Y., YOSHIKAWA, K., AND YOKOCHI, T. A new sensitive and rapid automated fluorometric assay for detection of natural killer activity using carboxyfluorescein diacetate. *J. Immunoassay* 12: 145–157, 1991.

SWARTZ, K. J. Modulation of Ca^{2+} channels by protein kinase C in rat central and peripheral neurons: disruption of G protein-mediated inhibition. *Neuron* 11: 305–320, 1993.

TANABE, Y., MASU, M., ISII, T., SHIGEMOTO, R., NAKANISHI, S. A family of metabotropic glutamate receptors. *Neuron* 8: 169–179, 1992.

TAYLOR, C. W. AND MARSHALL, I. C. B. Calcium and inositol-1,4,5-trisphosphate receptors: a complex relationship. *Trends Biochem. Sci.* 17: 403–407, 1992.

THOMPSON, A. K., MOSTAFAPOUR, S. P., DENLINGER, L. C., BLEASDALE, J. E., AND FISHER, S. K. The aminosteroid U-73122 inhibits muscarinic receptor sequestration and phosphoinositide hydrolysis in SK-N-SH neuroblastoma cells. *J. Biol. Chem.* 266: 23856–23862, 1991.

TOULLEC, D., PIANETTI, P., COSTE, H., BELLEVERGUE, P., GRAND-PERRETT, T., AJAKANES, M., BAUDET, V., BOISSIN, P., BOURSIER, E., LORIOLLE, F., DUHAMEL, L., CHARON, D., AND KIRILOVSKY J. The bisindolymaleimide GF 109203X is a potent and selective inhibitor of protein kinase C. *J. Biol. Chem.* 266: 15771–15781, 1991.

TYMIANSKI, M., CHARLTON, M. P., CARLEN, P. L., AND TATOR, C. H. Source specificity of early calcium neurotoxicity in cultured embryonic spinal neurons. *J. Neurosci.* 13: 2085–2104, 1993.

VOLPE, P. AND ALDERSON-LANG, B. H. Regulation of inositol-1,4,5-trisphosphate-induced Ca^{2+} release II. Effect of cAMP-dependent protein kinase. *Am. J. Physiol.* 258 (*Cell Physiol.* 27): C1086–C1091, 1990.

VORNOV, J. J., TASKER, R. C., AND COYLE, J. T. Direct observation of the agonist-specific regional vulnerability to glutamate, NMDA, and kainate neurotoxicity in organotypic hippocampal cultures. *Exp. Neurol.* 114: 11–22, 1991.

VYKLICKY, L. J. Calcium-mediated modulation of *N*-methyl-D-aspartate (NMDA) responses in cultured rat hippocampal neurons. *J. Physiol. (Lond.)* 470: 575–600, 1993.

WAKADE, A. R., WAKADE, T. D., MALHOTRA, R. K. AND BHAVE, S. J. Excess K^+ and phorbol ester activate protein kinase C and support the survival of chick sympathetic neurons in culture. *J. Neurochem.* 51: 975–983, 1988.

WANG, L.-Y., SALTER, M. W., AND MACDONALD J. F. Regulation of kainate receptors by cAMP-dependent protein kinase and phosphatases. *Science* 253: 1132–1135, 1991.

WARCHOL, M. E. AND DALLOS P. Neural coding in the chick cochlear nucleus. *J. Comp. Physiol.* [*A*] 166: 721–734, 1990.

WESTERBERG, B. D. AND SCHWARZ, D.W.F. Connections of the superior olive in the chicken. *J. Otolaryngol.* 24: 20–30, 1995.

WIESEL, T. N. AND HUBEL, D. H. Effects of visual deprivation on morphology and physiology of cells in the cat's lateral geniculate body. *J. Neurophysiol.* 26: 978–993, 1963a.

WIESEL, T. N. AND HUBEL, D. H. Single cell responses in striate cortex of kittens deprived of vision in one eye. *J. Neurophysiol.* 26: 1003–1017, 1963b.

WILDE, G.J.C., SUNDSTROM, L. E., AND IANOTTI, F. Propidium iodide in vivo: an early marker of neuronal damage in rat hippocampus. *Neurosci. Letters* 180: 223–226, 1994.

WOOLF, N. K., SHARP, F. R., DAVIDSON, T. M., AND RYAN, A. F. Cochlear and middle ear effects on metabolism in the central auditory pathway during silence: a 2-deoxyglucose study. *Brain Res.* 274: 119–127, 1983.

WYLLIE, A. H., MORRIS, R. G., SMITH, A. L., AND DUNLOP, D. Chromatin cleavage in apoptosis: association with condensed chromatin morphology and dependence on macromolecular synthesis. *J. Pathol.* 142: 67–77, 1984.

ZHOU, N. AND PARKS, T. N. Developmental changes in the effects of drugs acting at NMDA or non-NMDA receptors on synaptic transmission in the chick cochlear nucleus (nuc. magnocellularis). *Dev. Brain Res.* 67: 145–152, 1992a.

ZHOU, N. AND PARKS, T. N. γ-D-glutamylaminomethyl sulfonic acid (GAMS) distinguishes subtypes of glutamate receptors in the chick cochlear nucleus (nuc. magnocellularis). *Hear. Res.* 60: 20–26, 1992b.

ZHOU, N., TAYLOR, D. A., AND PARKS, T. N. Cobalt-permeable non-NMDA receptors in developing chick brainstem auditory nuclei. *Neuroreport* 6: 2273–2276, 1995.

ZIRPEL, L., LACHICA, E. A., AND LIPPE, W. R. Deafferentation increases the intracellular calcium of cochlear nucleus neurons in the embryonic chick. *J. Neurophysiol.* 74: 1355–1357, 1995a.

ZIRPEL, L., LACHICA, E. A., AND RUBEL, E. W Activation of a metabotropic glutamate receptor increases intracellular calcium concentrations in neurons of the avian cochlear nucleus. *J. Neurosci.* 15: 214–222, 1995b.

ZIRPEL, L., LACHICA, E. A., AND RUBEL, E. W Afferent regulation of neurons in the avian cochlear nucleus: intracellular mechanisms and signal transduction pathways. In: *Neurotransmission and Hearing Loss: Basic Science, Diagnosis and Management*, San Diego, CA: Singular Publishing Group, 1997, p. 47–76.

ZIRPEL, L., NATHANSON, N. M., RUBEL, E. W, AND HYSON, R. L. Glutamate stimulated phosphatidylinositol metabolism in the avian cochlear nucleus. *Neurosci. Lett.* 168: 163–168, 1994.

ZIRPEL, L., AND RUBEL, E. W Eighth nerve activity regulates the intracellular calcium concentration of avian cochlear nucleus neurons via a metabotropic glutamate receptor. *J. Neurophysiol.* 76: 4127–4139, 1996a.

ZIRPEL, L. AND RUBEL, E. W Role of Protein Kinases A and C in Activity-dependent Regulation of $[Ca^{2+}]_i$ in Avian Cochlear Nucleus Neurons. *Soc. Neurosci. Abstr.* 22: 401, 1996b.

ZONG, X. AND LUX, H. D. Augmentation of calcium channel currents in response to G-protein activation by GTPγS in chick sensory neurons. *J. Neurosci.* 14: 4847–4853, 1994.